LEVEL II 12

SDAC-TR-77-6

STUDY OF SELECTED EVENTS IN THE CAUCASUS IN A SEISMIC DISCRIMINATION CONTEXT

P.A. SOBEL, D.H. VON SEGGERN, E.I. SWEETSER & D.W. RIVERS

Seismic Data Analysis Center

Teledyne Geotech, 314 Montgomery Street, Alexandria, Virginia 22314

07 NOVEMBER 1977

Sponsored by

The Defense Advanced Research Projects Agency (DARPA)

ARPA Order No. 2551

Monitored By

AFTAC/VSC

312 Montgomery Street, Alexandria, Virginia 22314

Disclaimer: Neither the Defense Advanced Research Projects Agency nor the Air Force Technical Applications Center will be responsible for information contained herein which has been supplied by other organizations or contractors, and this document is subject to later revision as may be necessary. The views and conclusions presented are those of the authors and should not be interpreted as necessarily representing the official policies, either expressed or implied, of the Defense Advanced Research Projects Agency, the Air Force Technical Applications Center, or the US Government.

Unclassified

SECURITY CLASSIFICATION OF THIS PAGE (When Data Entered)

REPORT DOCUMENTATION PAGE

READ INSTRUCTIONS BEFORE COMPLETING FORM

1. REPORT NUMBER: SDAC-TR-77-6	2. GOVT ACCESSION NO.
3. RECIPIENT'S CATALOG NUMBER	
4. TITLE (and Subtitle): STUDY OF SELECTED EVENTS IN THE CAUCASUS IN A SEISMIC DISCRIMINATION CONTEXT.	5. TYPE OF REPORT & PERIOD COVERED: Technical rept.
	6. PERFORMING ORG. REPORT NUMBER
7. AUTHOR(s): P. A. Sobel, E. I. Sweetser, D. H. von Seggern, D. W. Rivers	8. CONTRACT OR GRANT NUMBER(s): F08606-78-C-0007, ARPA Order-2551
9. PERFORMING ORGANIZATION NAME AND ADDRESS: Teledyne Geotech, 314 Montgomery Street, Alexandria, Virginia 22314	10. PROGRAM ELEMENT, PROJECT, TASK AREA & WORK UNIT NUMBERS: VT/8709
11. CONTROLLING OFFICE NAME AND ADDRESS: Defense Advanced Research Projects Agency, Nuclear Monitoring Research Office, 1400 Wilson Blvd. Arlington, Virginia 22209	12. REPORT DATE: 7 Nov 77
	13. NUMBER OF PAGES: 68
14. MONITORING AGENCY NAME & ADDRESS (if different from Controlling Office): VELA Seismological Center, 312 Montgomery Street, Alexandria, Virginia 22314	15. SECURITY CLASS. (of this report): Unclassified
	15a. DECLASSIFICATION/DOWNGRADING SCHEDULE

16. DISTRIBUTION STATEMENT (of this Report)

APPROVED FOR PUBLIC RELEASE; DISTRIBUTION UNLIMITED.

17. DISTRIBUTION STATEMENT (of the abstract entered in Block 20, if different from Report)

18. SUPPLEMENTARY NOTES

Author's Report Date 06/13/77

19. KEY WORDS (Continue on reverse side if necessary and identify by block number)

Seismic Discrimination
$M_s - m_b$
Caucasus Earthquakes
Kazakh Explosions
Seismic Attenuation
Seismic Source Spectrum

M sub S M sub b

20. ABSTRACT (Continue on reverse side if necessary and identify by block number)

Eight earthquakes from the Caucasus occurring from 1971 to 1975 were examined in a seismic discrimination context. Seismograms from ALPA, LASA, NORSAR, and the HGLP and the WWSSN stations were studied for source mechanism, $M_s - m_b$, corner frequency, pP, complexity, and spectral ratio. All the Caucasus events can be identified as earthquakes by means of pP and $M_s : m_b$ when compared to Kazakh and southwest USSR explosions. However it seems plausible that these discriminants could be rendered ineffective for events in the Caucasus by means of a shot array.

DD FORM 1 JAN 73 1473 EDITION OF 1 NOV 65 IS OBSOLETE

M sub S ! M sub b

Unclassified

SECURITY CLASSIFICATION OF THIS PAGE (When Data Entered)

408 258

STUDY OF SELECTED EVENTS IN THE CAUCASUS IN A SEISMIC DISCRIMINATION CONTEXT

SEISMIC DATA ANALYSIS CENTER REPORT NO.: SDAC-TR-77-6

AFTAC Project Authorization No.: VELA T/8709/B/ETR

Project Title: Seismic Data Analysis Center

ARPA Order No.: 2551

Name of Contractor: TELEDYNE GEOTECH

Contract No.: F08606-78-C-0007

Date of Contract: 01 Oct 1977

Amount of Contract: $2,674,245

Contract Expiration Date: 30 Sep 1978

Project Manager: Robert R. Blandford
(703) 836-3882

P. O. Box 334, Alexandria, Virginia 22314

ABSTRACT

Eight earthquakes from the Caucasus occurring from 1971 to 1975 were examined in a seismic discrimination context. Seismograms from ALPA, LASA, NORSAR, and the HGLP and the WWSSN stations were studied for source mechanism, M_s-m_b, corner frequency, pP, complexity, and spectral ratio. All the Caucasus events can be identified as earthquakes by means of pP and M_s:m_b when compared to Kazakh and southwest USSR explosions. However it seems plausible that these discriminants could be rendered ineffective for events in the Caucasus by means of a shot array.

TABLE OF CONTENTS

	Page
ABSTRACT	2
LIST OF FIGURES	4
LIST OF TABLES	6
INTRODUCTION	7
TECTONIC SETTING	8
General Features	8
Source Mechanisms of Earthquakes	8
Velocity Model	8
DATA	12
Explosion Selection	12
Seismic Stations	12
SIGNAL ANALYSIS	15
Source Effects	15
Propagation Effects	37
DISCRIMINATION ASPECTS	54
$M_s - m_b$	54
Corner Frequency and Long-Period Spectral Level	58
Long-Period Body-Wave Excitation	60
Depth of Focus	60
Complexities	60
Spectral Ratios	62
Radiation Pattern	62
S/P Excitation	65
SUMMARY	66
REFERENCES	67

LIST OF FIGURES

Figure No.	Title	Page
1	Map of Caucasus showing faults observed on satellite photographs and NEIS epicenters from January 1971 through February 1975.	9
2	LASA and NORSAR short-period P recordings for the Caucasus events studied.	14
3	First motions for Caucasus earthquakes in the lower half of the focal sphere (Wulff net).	16
4	LASA A0 and NORSAR C3 subarray spectra of P waves from Caucasus earthquakes with instrument response and attenuation removed.	24
5	Seismic moment versus corner frequency for Caucasus earthquakes from LASA and NORSAR P recordings.	38
6	Observed LR amplitudes (T = 20 sec) for Caucasus event 7.	43
7	Average of all short-period P spectra for the path Caucasus to LASA.	45
8	Average of all short-period P spectra for the path Caucasus to NORSAR.	46
9	Ln(F) + 2·ln(f) versus frequency for the path Caucasus to LASA.	47
10	Ln(F) + 3·ln(f) versus frequency for the path Caucasus to LASA.	48
11	Ln(F) + 2·ln(f) versus frequency for the path Caucasus to NORSAR.	49
12	Ln(F) + 3·ln(f) versus frequency for the path Caucasus to NORSAR.	50
13	Predicted LR raypaths (T = 20 sec) for event 7 (42.9N, 47.0E).	52
14	M_s vs. m_b for Caucasus earthquakes and Kazakh and southwest USSR explosions.	57

LIST OF FIGURES (Continued)

Figure No.	Title	Page
15	Long-period spectral level vs. corner frequency for Caucasus earthquakes and Kazakh and southwest USSR explosions from LASA and NORSAR P recordings.	59
16	Complexity vs. m_b for Caucasus earthquakes and Kazakh and southwest USSR explosions from LASA and NORSAR P recordings.	61
17	Short-period P spectral ratio uncorrected for attenuation vs. m_b for Caucasus earthquakes and Kazakh and southwest USSR explosions recorded at LASA and NORSAR.	63
18	Short-period P spectral ratio corrected for attenuation vs. m_b for Caucasus earthquakes and Kazakh and southwest USSR explosions recorded at LASA and NORSAR. The t* values are for ω^{-2} source models for earthquakes and explosions and ω^{-3} source models for earthquakes.	64

LIST OF TABLES

Table No.	Title	Page
I	Velocity Structure in the Caucasus	11
II	NEIS Parameters for Caucasus Earthquakes	13
III	NEIS Parameters for Kazakh and Southwest USSR Explosions	13
IV	Magnitude Data for Caucasus Earthquakes	39
V	Magnitude Data for Kazakh and Southwest USSR Explosions	55

INTRODUCTION

Discrimination parameters have been applied in detail to events from only a few nuclear test sites and earthquake regions. This study is part of a series which extends these discrimination studies to other regions of shallow earthquakes. This particular report examines eight such earthquakes in the Caucasus of the USSR. Most of the earthquakes in the Caucasus are probably associated with large thrust faults, which are a result of the Meso-Cenozoic Alpine orogeny. Actual seismogram analysis revealed that the events chosen were too small to determine their fault plane solutions. We determine average M_s and m_b for the events in this study and apply other common discrimination parameters such as first motions, corner frequency, complexity, and short-period spectral ratios to the data. Results for the Caucasus events will be compared to Kazakh and USSR explosions.

TECTONIC SETTING

General Features

Figure 1 is a map of the Caucasus region. The principal geologic features in this area trend northwest-southeast and are associated with the Meso-Cenozoic Alpine orogeny. In general the seismicity follows the trend of the mountains, but zones of higher activity occur near 43N, 47E and 41N, 48E (Nowroozi, 1971). In general the seismicity is well enough distributed that no area is exempt from high seismic risk according to the Russian observations summarized in Byus et al. (1968). The majority of the earthquakes occur within the crust in the Caucasus Mountains (Keilis-Borok, 1960; Byus et al., 1968; Nowroozi, 1971); but where the seismic zone extends into the Caspian Sea, the earthquakes are subcrustal, with depths ranging from 50 to 150 km. These deeper events are possibly due to the subsidence of the Caspian Basin which has accumulated as much as 20 km of sediment in its southern portion.

Source Mechanisms of Earthquakes

NEIS epicenters for events in this area from January 1971 through February 1975 are shown in Figure 1. The geologic faults in this figure were inferred from a satellite photomosaic of the area. Most earthquakes are associated with thrust faults in this fold belt since compressional axes determined from fault-plane solution are generally perpendicular to the trend of the geologic structure (Keilis-Borok, 1960; Nowroozi, 1971). Within this dominant NW-SE strike, there is considerable variance to the fault-plane orientations; and strike-slip motion is not uncommon.

Velocity Model

Deep seismic sounding studies report crustal thicknesses reaching 50 to 60

Nowroozi, A., 1971. Seismo-tectonics of the Persian Plateau, Eastern Turkey Caucasus, and Hindu-Kush Regions, Bull. Seism. Soc. Am., 61, 317.

Byus, E. I., A. D. Tskhakaya, and M. M. Rubinshtein, 1968. Regional seismic zoning of the USSR: Georgia, in Seismic Zoning of the USSR, edited by S. V. Medvedev, English translation, Keter Publishing House, Jerusalem, Israel.

Keilis-Borok, V. I., 1960. Investigation of the Mechanism of Earthquakes, English translation, American Geophysical Union, Washington, D. C.

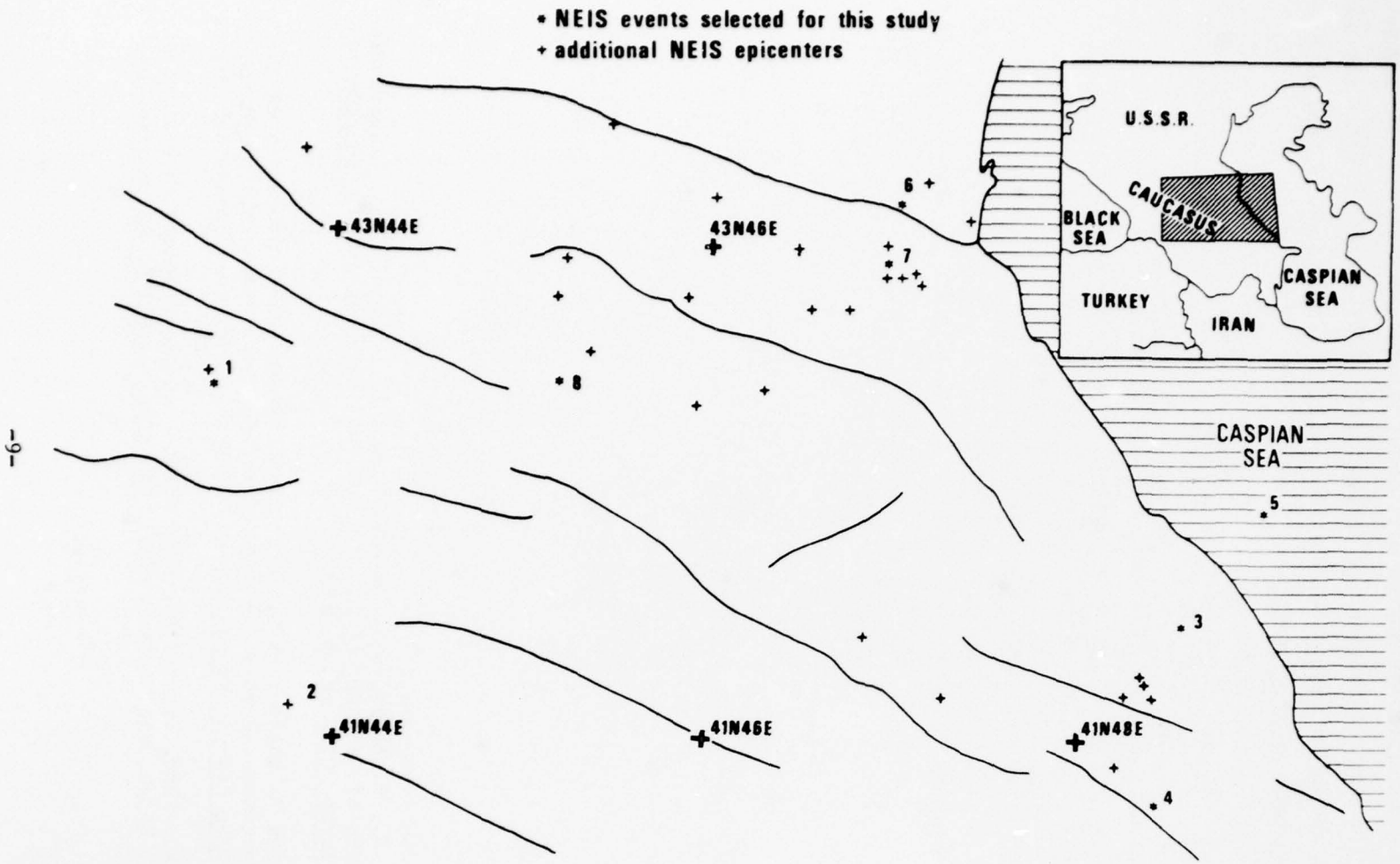

Figure 1. Map of Caucasus showing faults observed on satellite photographs and NEIS epicenters from January 1971 through February 1975.

km in the Caucasus (Beliayevsky et al., 1968; Borusk and Shalpo, 1976) and 35 to 40 km in the central Caspian Sea (Neprochnov, 1968). Table I shows the general crustal and upper mantle velocity structure for the Caucasus area of Figure 1 (Beliayevsky et al., 1968).

Beliayevsky, N., A. Borisov, I. Valvovsky, and Y. Schukin, 1968, Transcontinental crustal sections of the U.S.S.R. and adjacent areas, Canadian Journal of Earth Sciences, 5, 1967.

Borusk, A., and V. Shalpo, 1976, Correlation of endogenous processes in the Great Caucasus and adjacent part of the Scythian Platform, in Geodynamics: Progress and Prospects, ed. C. Drake, American Geophysical Union.

Neprochnov, H., 1968, Strucutre of the earht's crust of epicontinental seas: Caspian, Black, and Mediterranean, Canadian Journal of Earth Sciences, 5, 1037.

TABLE I

Velocity Structure in the Caucasus Mountains

Thickness (km)	P Velocity (km/sec))	Density (gm/cm^3)
20	5.6 - 6.0	2.7
35	6.9 - 7.4	3.1
mantle	8.1 - 8.2	3.3

DATA

Earthquake Selection

For this study shallow-focus earthquakes were selected from the Caucasus Mountains and Caspian Sea regions. The NEIS list suggests that the large majority of the earthquakes in the Caucasus mountains occur within the crust. Where the mountains extend into the Caspian Sea, the earthquakes are subcrustal, with depths ranging from 50 to 150 km. The earthquakes chosen were limited to the years 1971 to 1975 so that we could utilize the data from the large seismic arrays and the HGLP network. Initially, earthquakes with low M_s, relative to m_b, were sought; but a survey of available M_s data revealed no earthquakes with anomalously low M_s in this area for 1971-1975. Those earthquakes with the lowest observed M_s values, again relative to m_b, (NORSAR observations) were simply selected out. We selected a total of 8 earthquakes as listed in Table II and shown in Figure I. Table II also lists the depths determined from pP observations at LASA, NORSAR, and selected WWSSN stations. All of the selected events are located within the crust, except the Caspian Sea earthquake (event 5).

Explosion Selection

The Caucasus earthquakes were compared to explosions in Kazakh and southwest USSR which lie to the north and northeast of the Caucasus. We selected a total of 8 explosions as listed in Table III for this comparison.

Seismic Stations

Digital data from the three arrays ALPA, LASA, and NORSAR and from the available HGLP stations and film data from selected WWSSN stations were assembled for these events. WWSSN stations were selected on the basis of magnification and proximity to the region of study, and it is unlikely that stations not used here would significantly add to the data base for these Caucasus events.

The available LASA and NORSAR short-period P recordings are shown in Figure 2. We have used the AO subarray from LASA and the C3 subarray from NORSAR as in our previous reports of this series in order to avoid signal loss at high frequencies due to full-array beaming. The subarray beams have individual sensors delayed according to the appropriate velocity.

TABLE II

NEIS Parameters for Caucasus Earthquakes

Event	Date	Origin Time	LAT (N°)	LONG (°E)	m_b	Depth NEIS	Depth This Study
1	7106280	10:53:45.7	42.400	43.300	4.6	34	16
2	710908	22:35:15.8	41.100	43.800	4.8	33	16
3	711015	17:08:06.3	41.428	48.571	4.9	33	31
4	720203	02:29:21.9	40.719	48.403	5.1	39	23
5	731214	09:11:46.3	41.876	49.028	5.1	79	75
6	741223	05:22:08.4	43.128	47.049	4.9	33	33
7	750109	23:09:46.6	42.889	46.987	5.2	31	30
8	750220	14:44:25.6	42.431	45.179	4.8	33	23

TABLE III

NEIS Parameters for Kazakh and southwest USSR Explosions

Event	Date	Origin Time	LAT (°N)	LONG (°E)	m_b
1	711222	06 59 56.3	47.872	48.222	6.0
2	721003	08 59 57.8	46.848	45.010	5.8
3	721124	09 59 57.8	51.843	64.152	5.2
4	730815	01 59 57.8	42.711	67.410	5.3
5	730919	02 59 57.2	45.635	67.850	5.2
6	730930	04 59 57.5	51.608	54.582	5.2
7	740625	03 56 57.6	49.889	78.115	4.8
8	741207	05 59 56.9	49.908	77.648	4.8

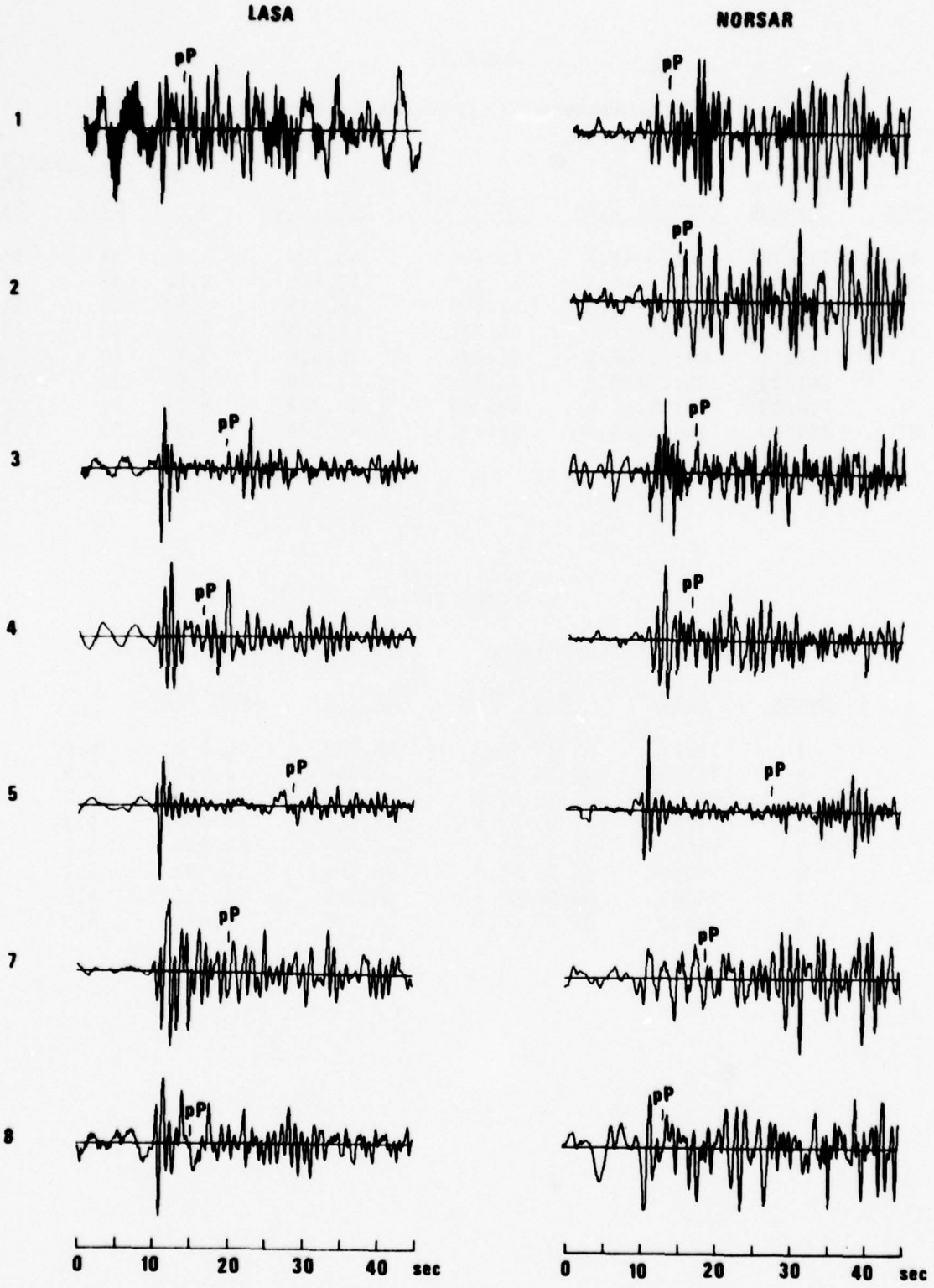

Figure 2. LASA and NORSAR short-period P recordings for the Caucasus events studied.

SIGNAL ANALYSIS

Source Effects

We wanted initially to identify a source mechanism for each event so that we could predict the radiation pattern for body-wave and surface-wave phases. Determination of the fault planes for earthquakes whose magnitudes are below 6.0 is generally not reliable with teleseismic data, and all our earthquakes have m_b less than 6. First motions were determined when possible from the data we had collected, and International Seismological Center (ISC) bulletin data was available for events 1 through 5. We have plotted all the first motions for the Caucasus earthquakes in Figure 3. Unfortunately, the short-period data were not consistent, and it is impossible on the basis of the plots alone to determine individual fault planes because dilatational and compressional first motions do not separate well. However, taken together, there is a dominance of compressional motion in the central to NE central part of the focal sphere plots; this would result from thrust faulting NE in a direction perpendicular to the trend of the Caucasus Mountains and is consonant with the body of known focal mechanisms for this region.

Corner frequencies and seismic moments for our Caucasus events have been estimated from short-period LASA and NORSAR spectra. The spectra are shown in Figure 4. These spectra are from the phased beams of the A0 subarray at LASA and C3 subarray at NORSAR. The sample length was 6.4 seconds. The signals have been tapered, and the instrument response was removed from the signal and noise spectra; but noise spectra have not been subtracted from the signal spectra. Attenuation was removed from the observed ($t^* = 0.0$) spectra by multiplying by the factor $\exp[\pi f t^*]$ with a t^* of .63 for a ω^{-2} source model and .44 for a ω^{-3} source model at LASA and t^* of .28 for ω^{-2} and .09 for ω^{-3} source models at NORSAR. The basis for these t^* values will be shown later in this report. Corner frequencies were estimated with the assumption of complete stress drop and a ω^{-2} or ω^{-3} asymptotic relation at high frequencies. Many of the estimates here of corner frequency and long-period level are tenuous, and those which were made with little confidence are represented by dashed lines in Figure 4. Occasionally we computed spectra for 256 second windows for those cases where the signal-to-noise ratio was adequate at lower frequencies. For these cases the shape of the spectra was sufficiently similar to those for the 6.4 second windows that we have not shown them.

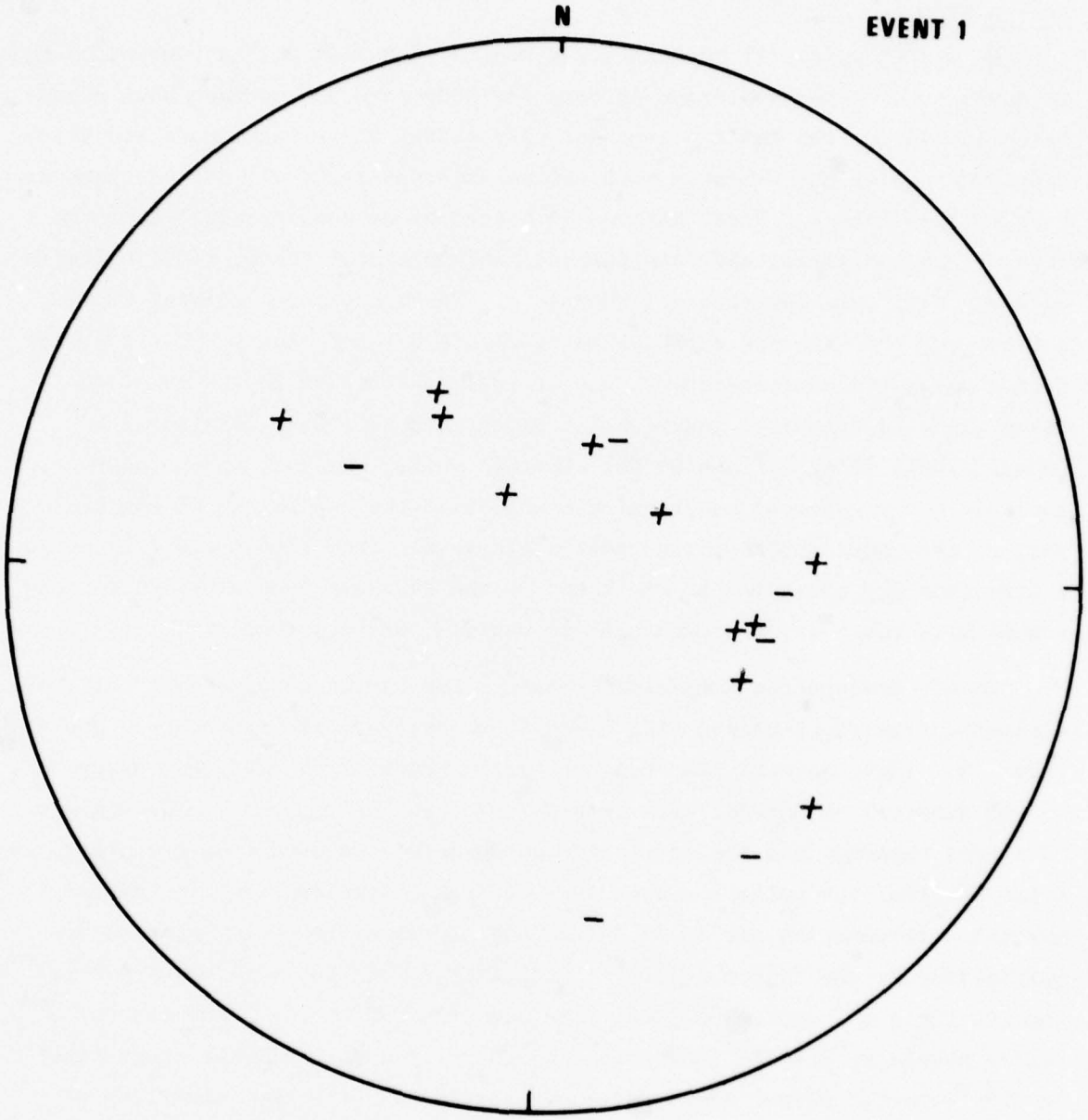

Figure 3. First motions for Caucasus earthquakes in the lower half of the focal sphere (Wulff net).

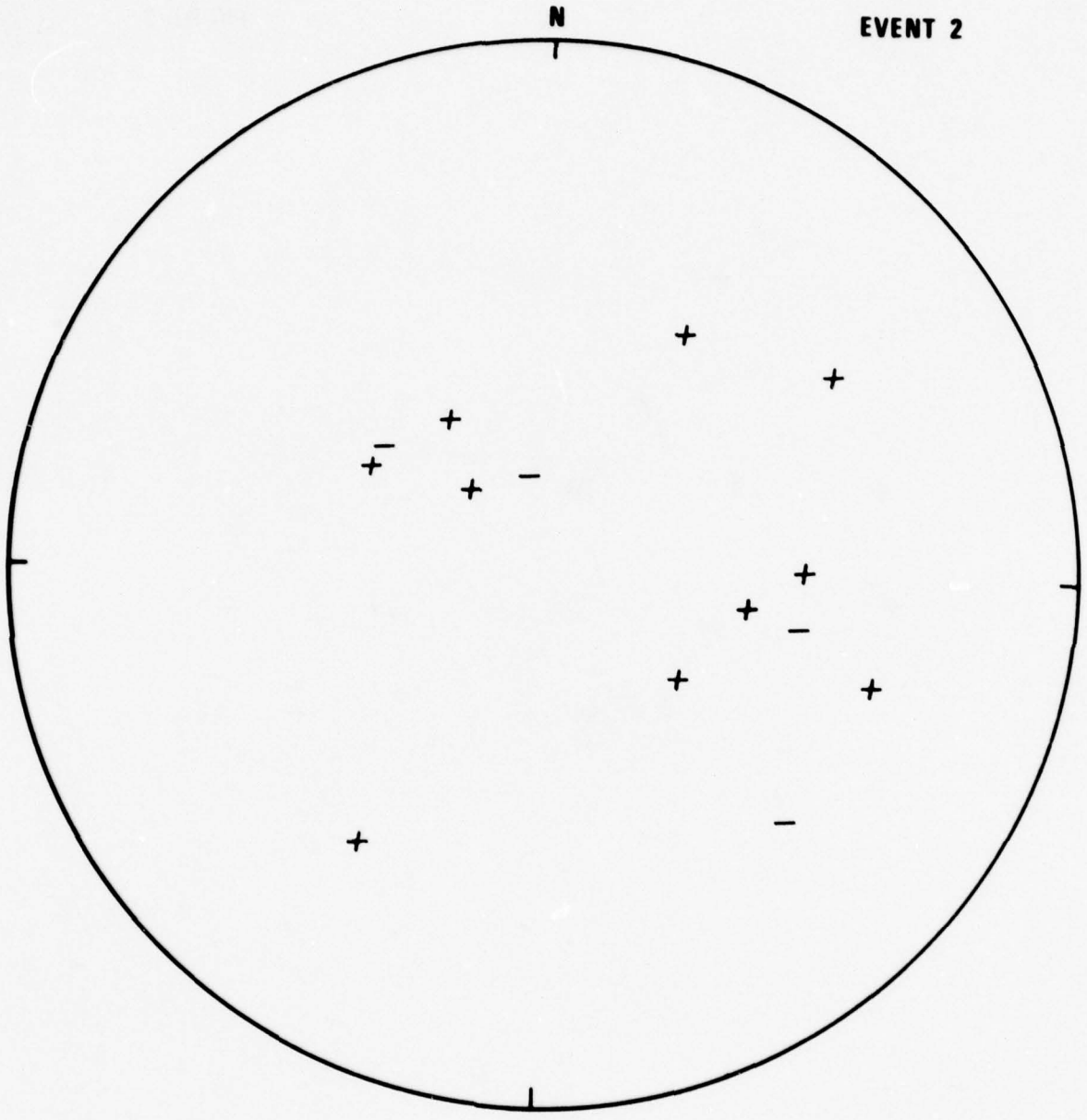

Figure 3 (cont.) First motions for Caucasus earthquakes in the lower half of the focal sphere (Wulff net).

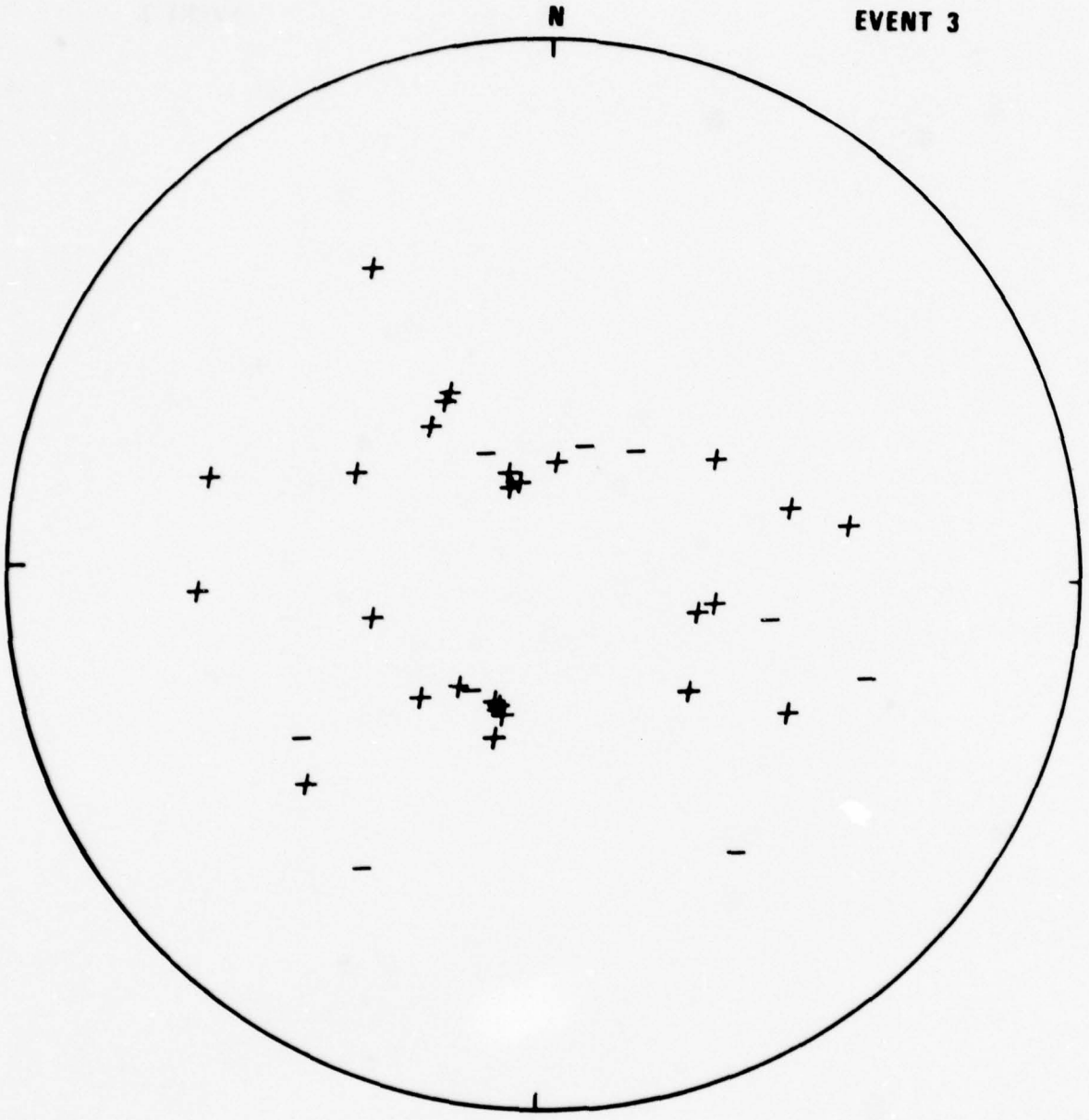

Figure 3 (cont.) First motions for Caucasus earthquakes in the lower half of the focal sphere (Wulff net).

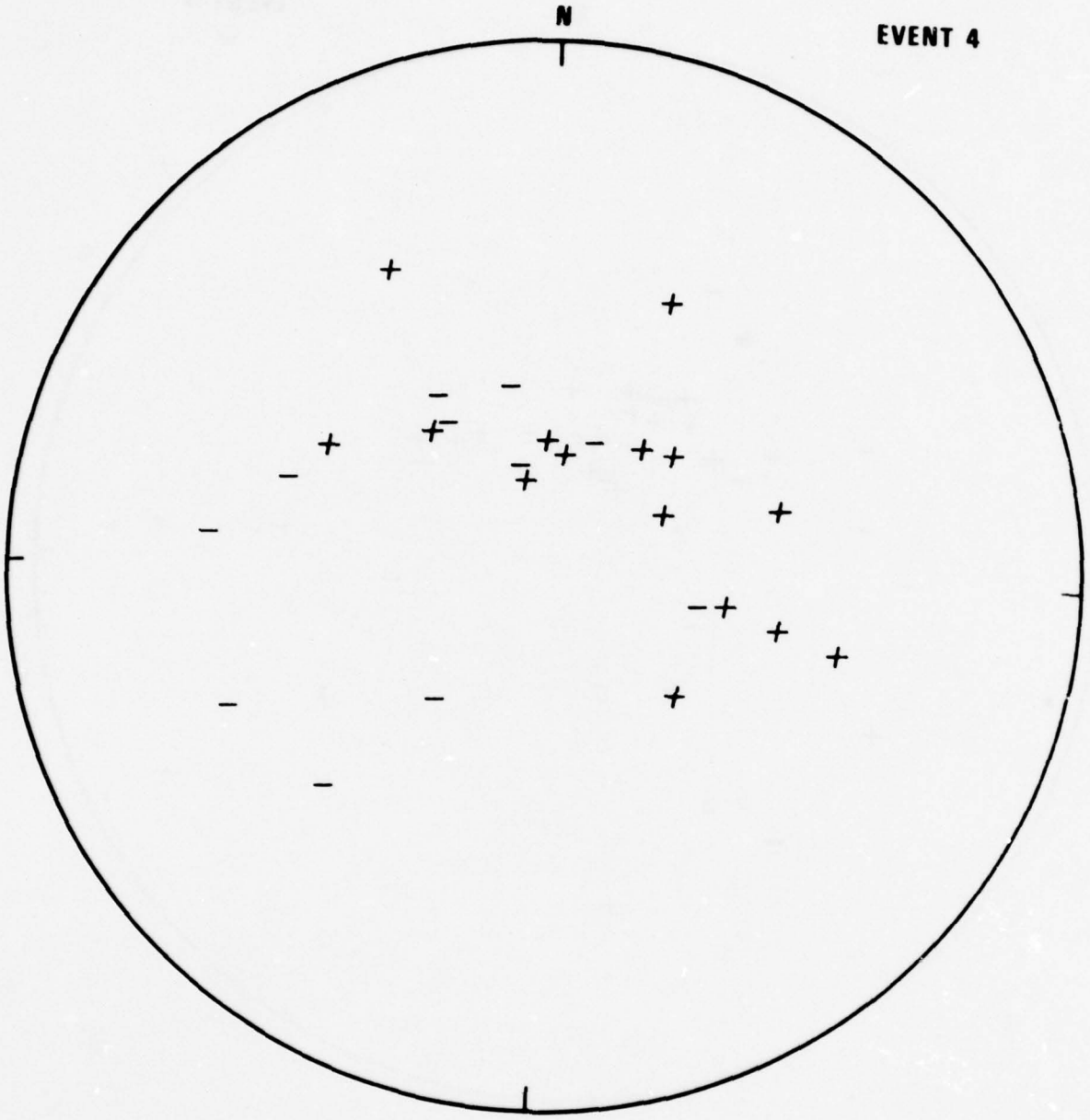

Figure 3 (cont.) First motions for Caucasus earthquakes in the lower half of the focal sphere (Wulff net).

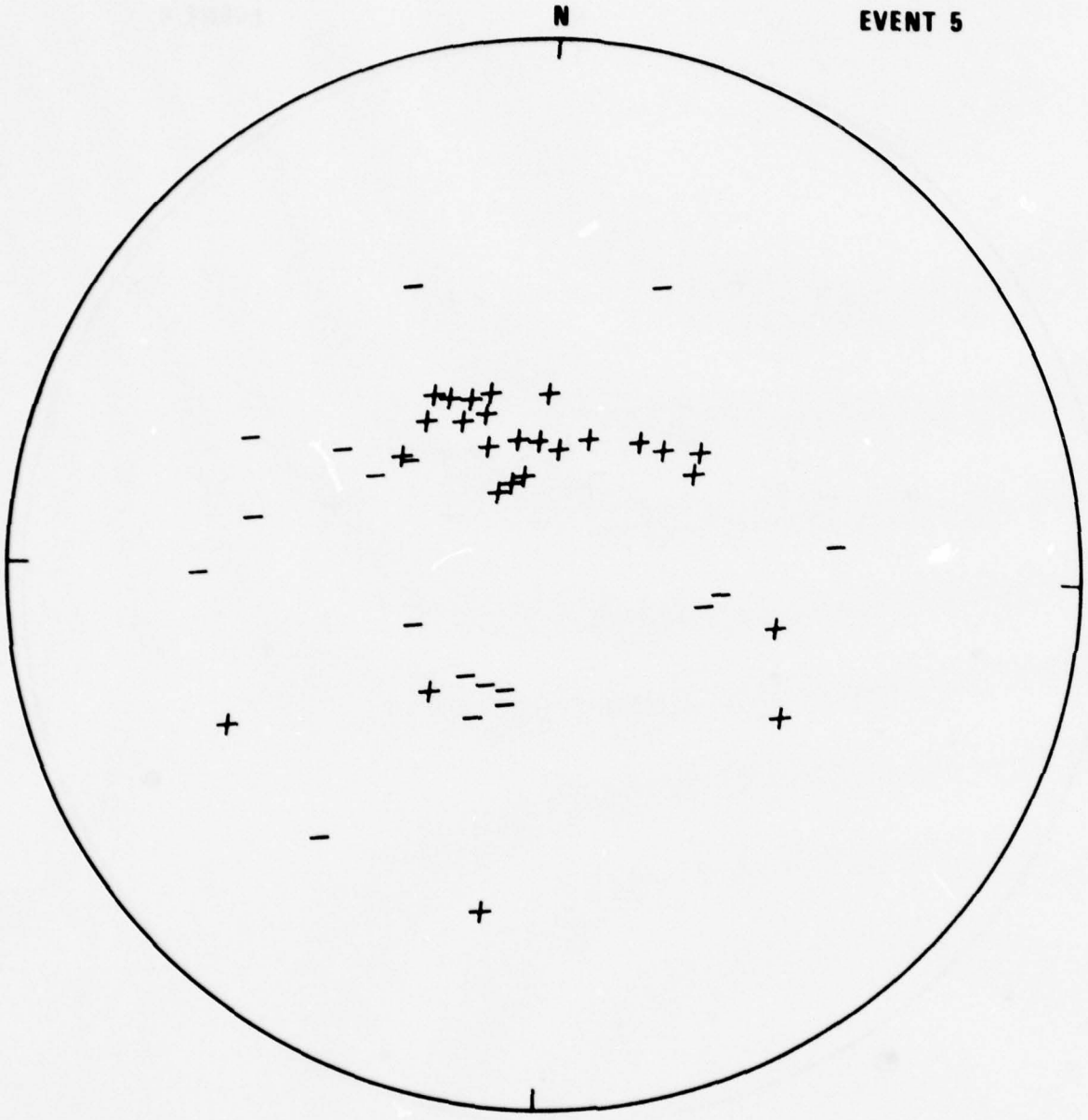

Figure 3 (cont.) First motions for Caucasus earthquakes in the lower half of the focal sphere (Wulff net).

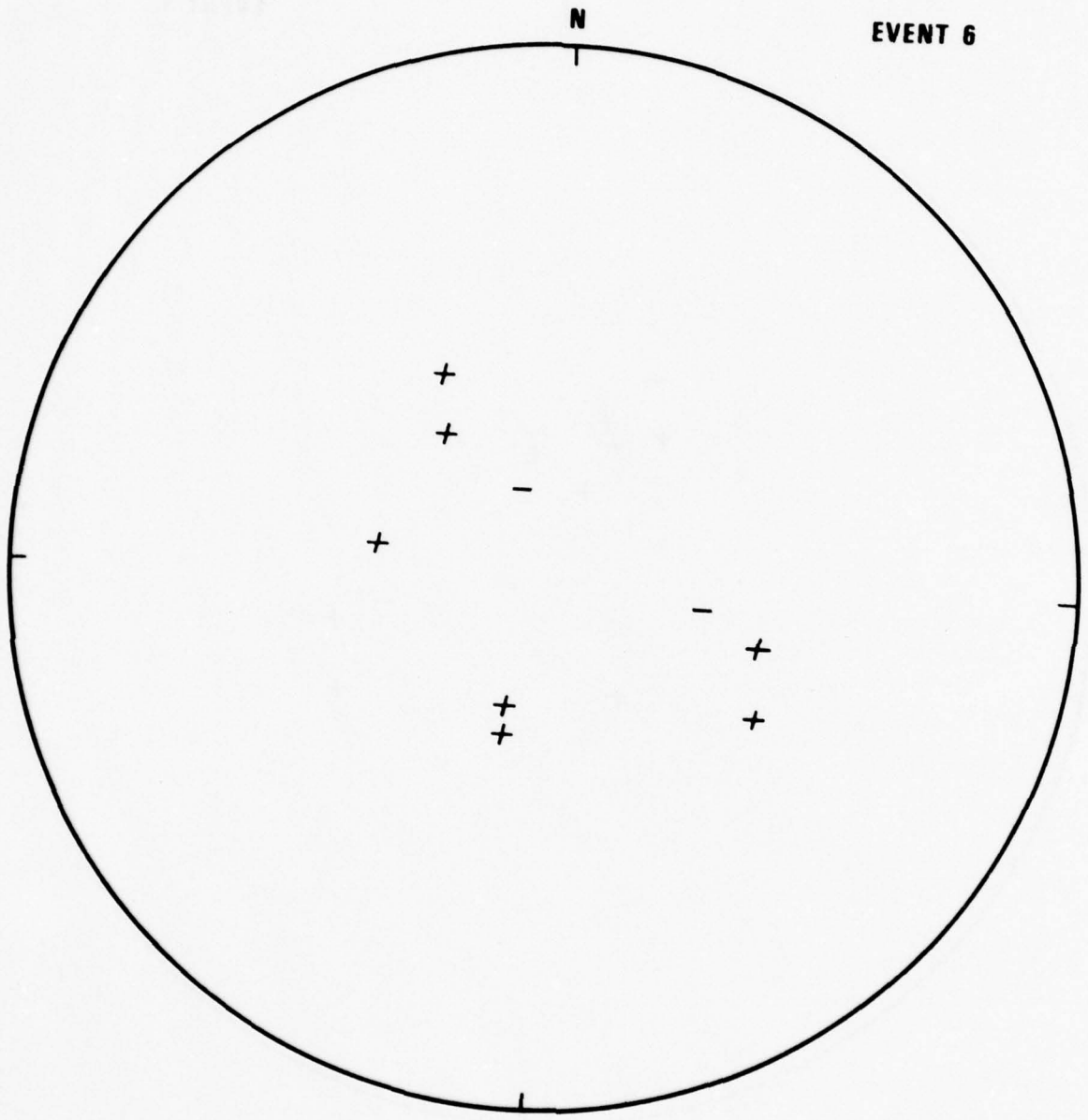

Figure 3 (cont.) First motions for Caucasus earthquakes in the lower half of the focal sphere (Wulff net).

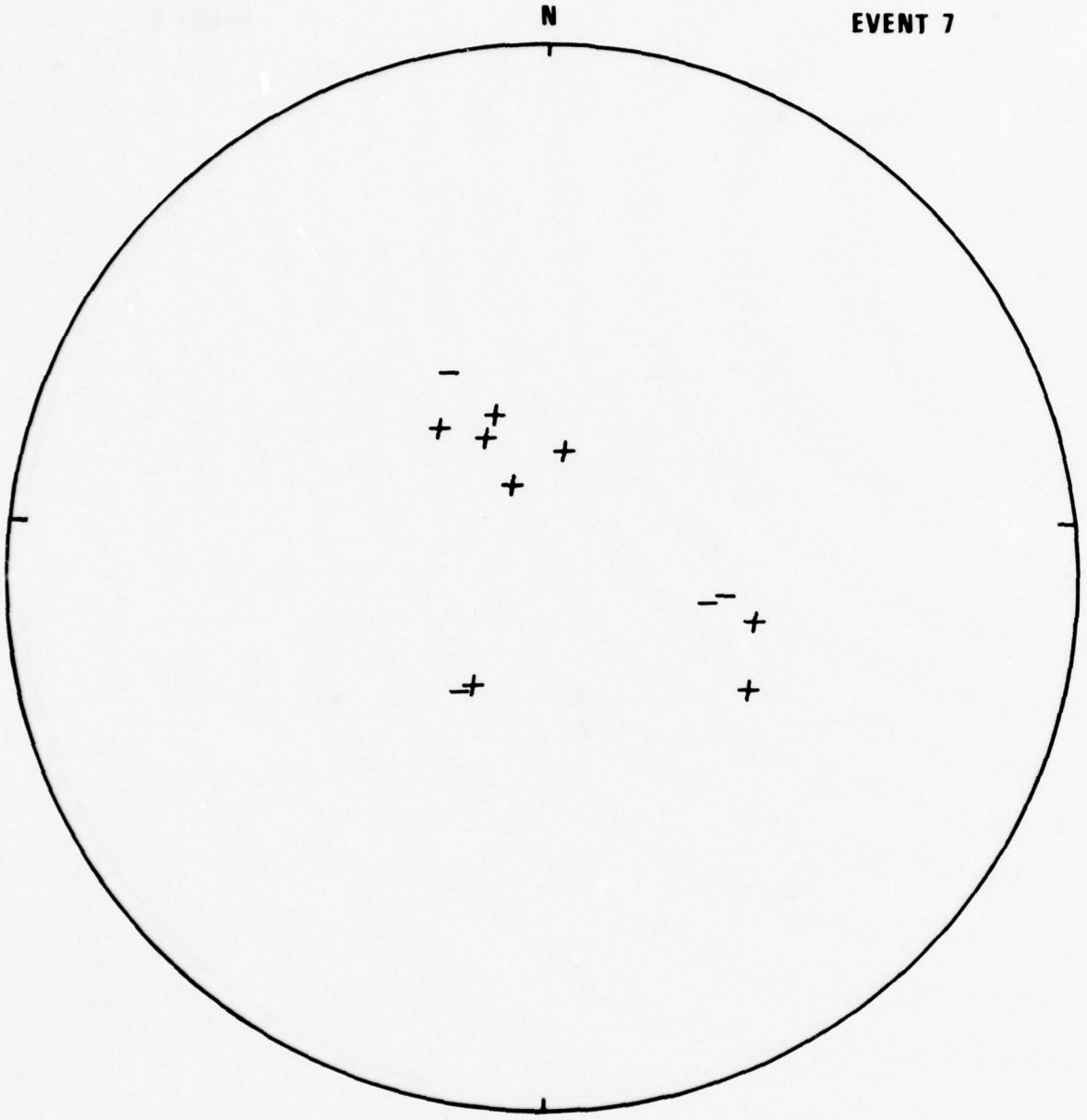

Figure 3 (cont.) First motions for Caucasus earthquakes in the lower half of the focal sphere (Wulff net).

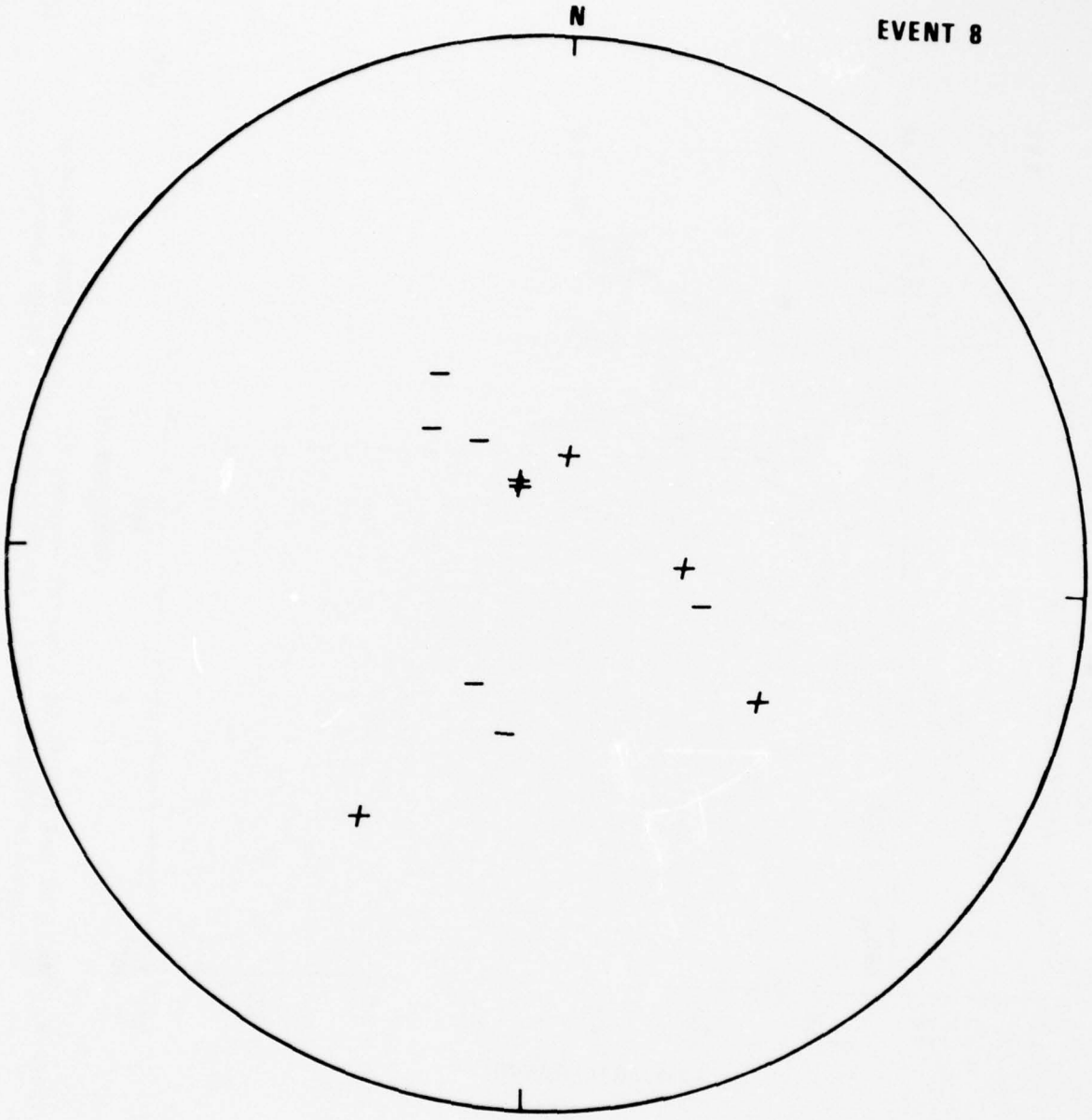

Figure 3 (cont.) First motions for Caucasus earthquakes in the lower half of the focal sphere (Wulff net).

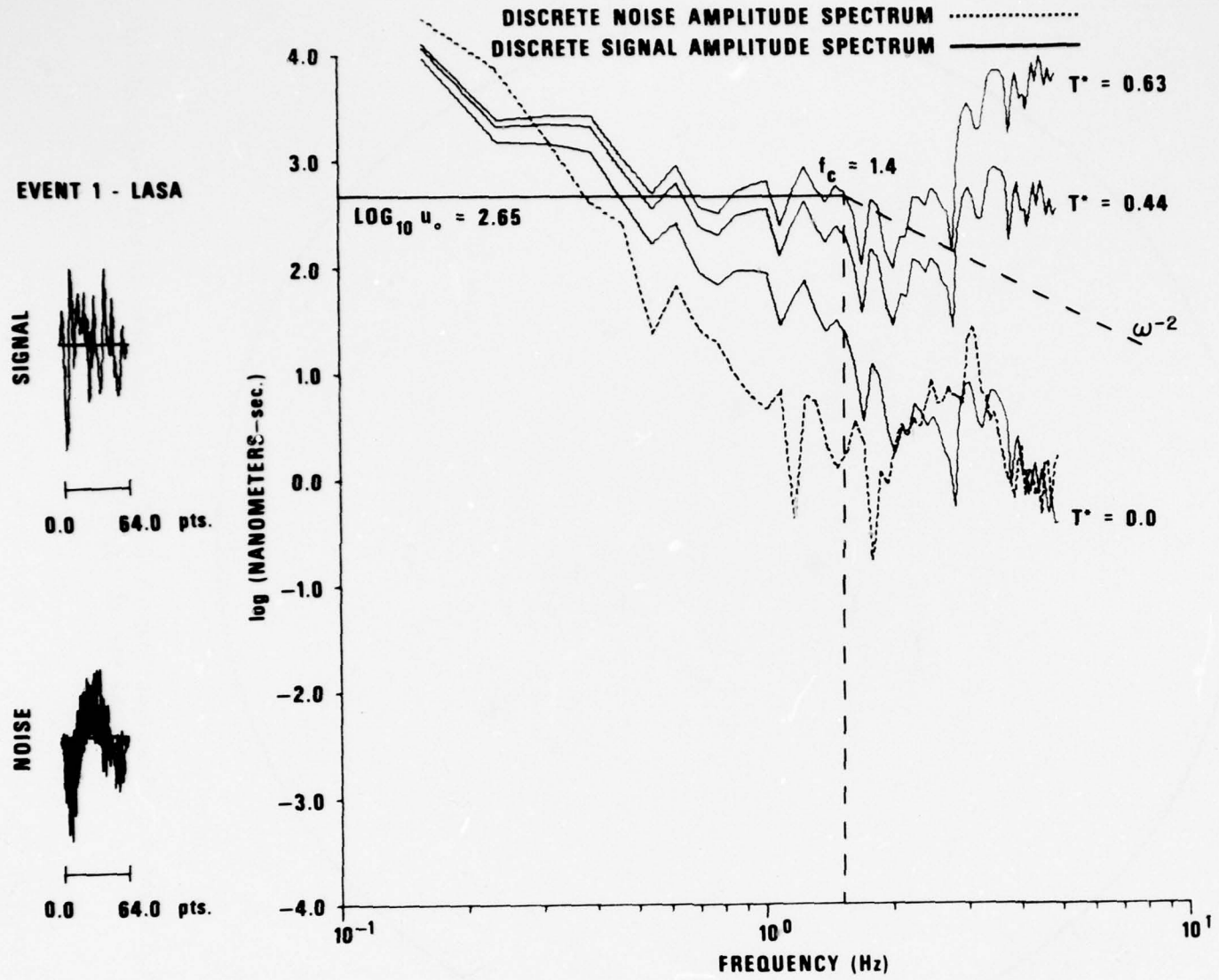

Figure 4. LASA AO and NORSAR C3 subarray spectra of P waves from Caucasus earthquakes with instrument response and attenuation removed.

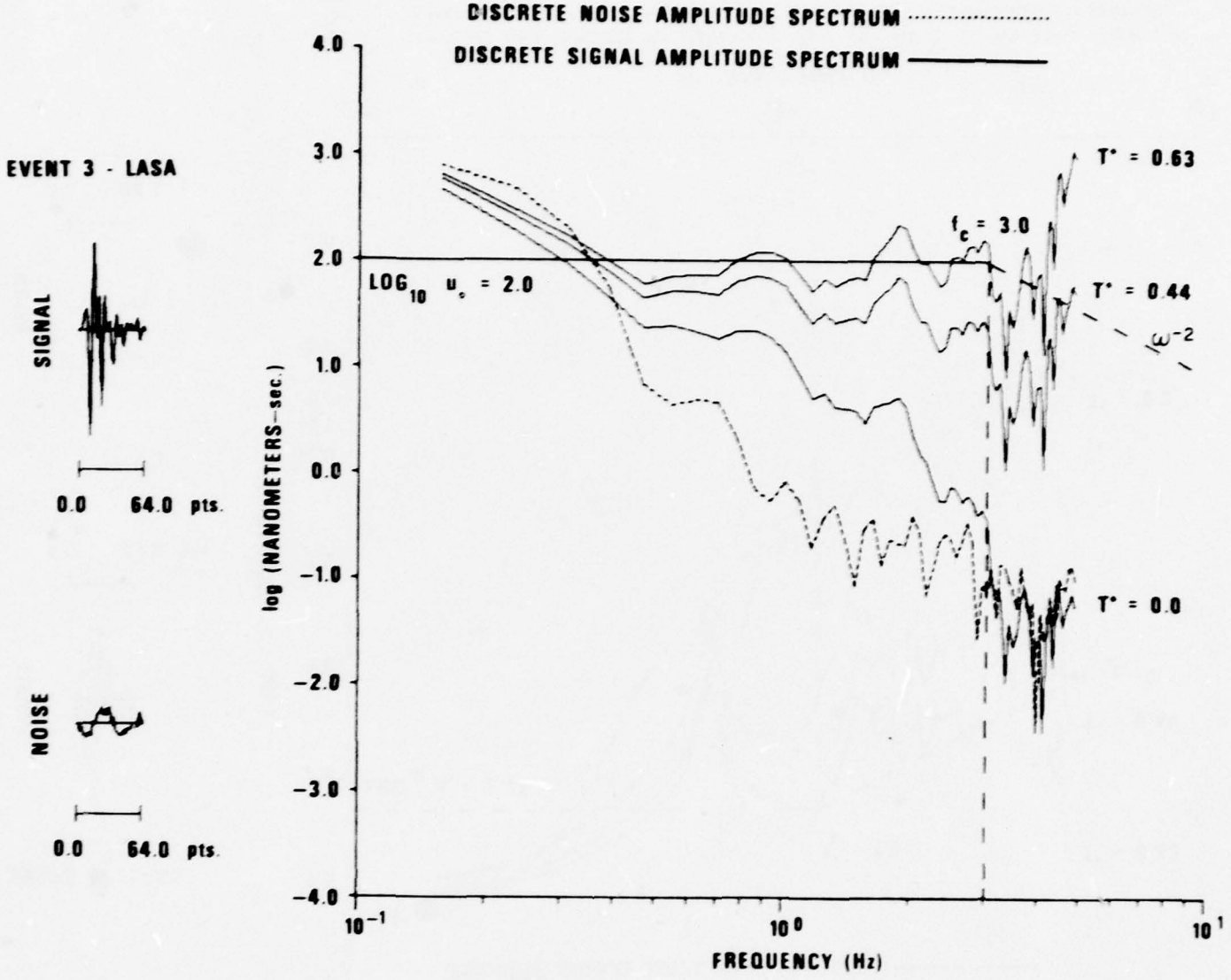

Figure 4 (cont.) LASA A0 and NORSAR C3 subarray spectra of P waves from Caucasus earthquakes with instrument response and attenuation removed.

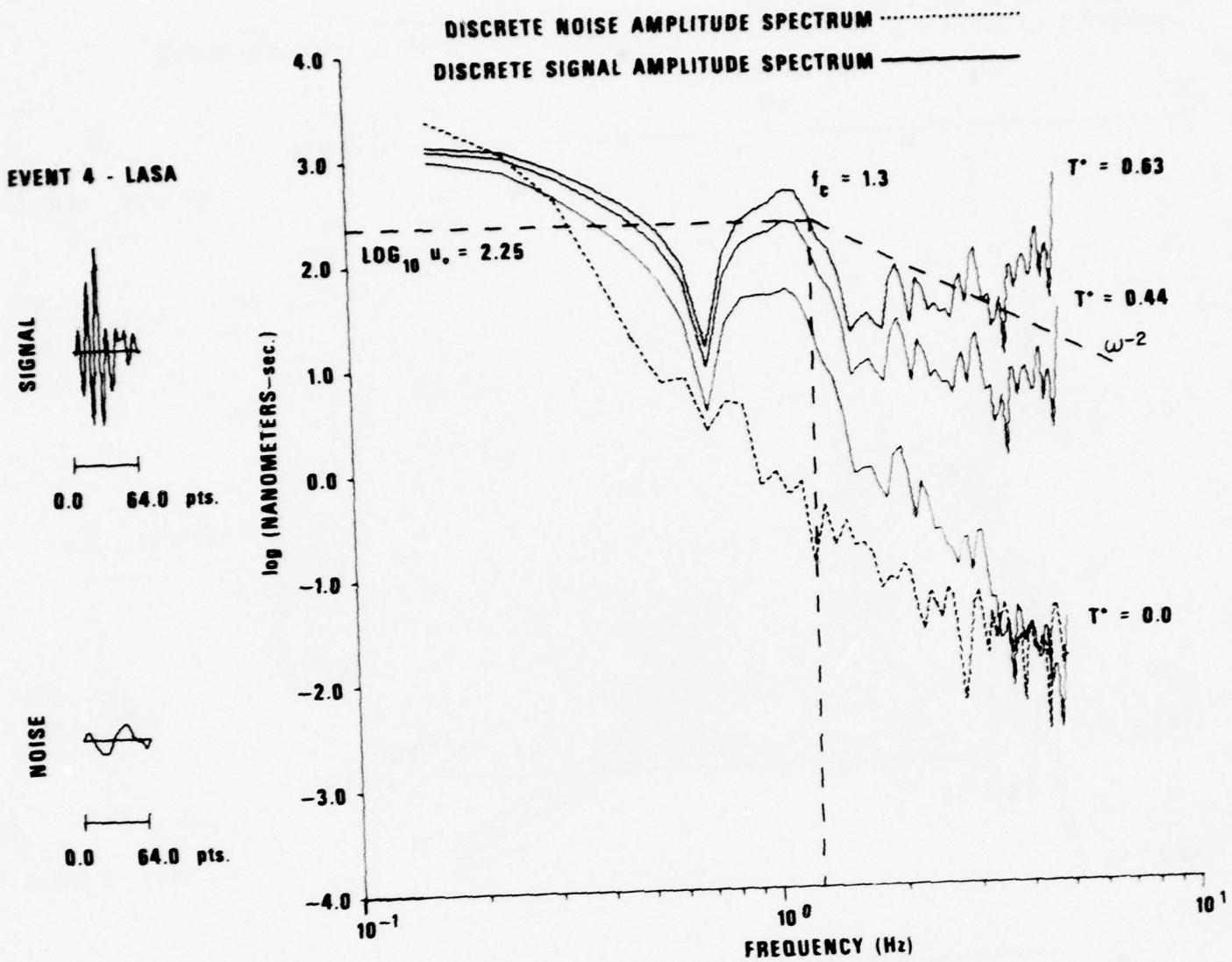

Figure 4 (cont.) LASA AO and NORSAR C3 subarray spectra of P waves from Caucasus earthquakes with instrument response and attenuation removed.

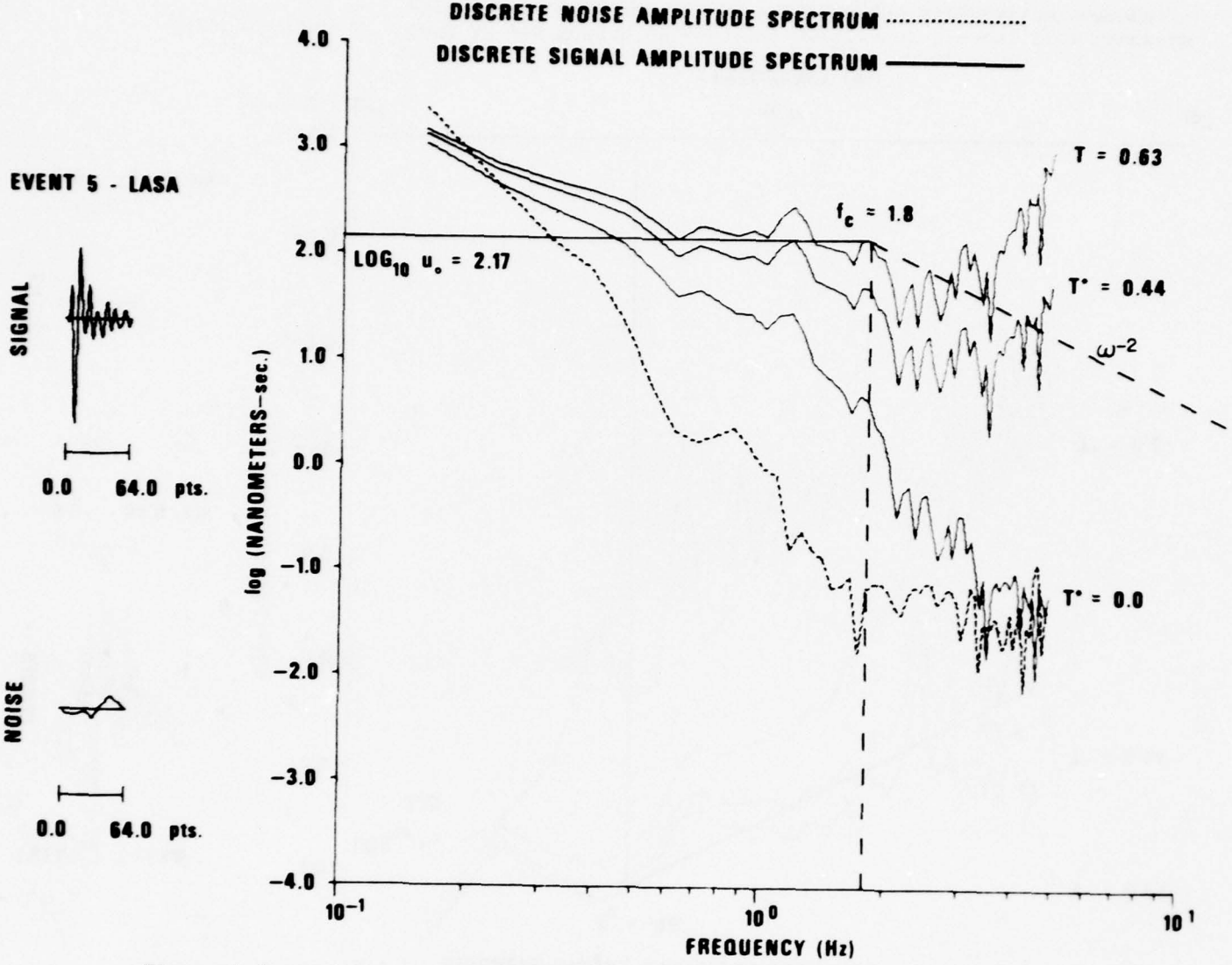

Figure 4 (cont.) LASA AO and NORSAR C3 subarray spectra of P waves from Caucasus earthquakes with instrument response and attenuation removed.

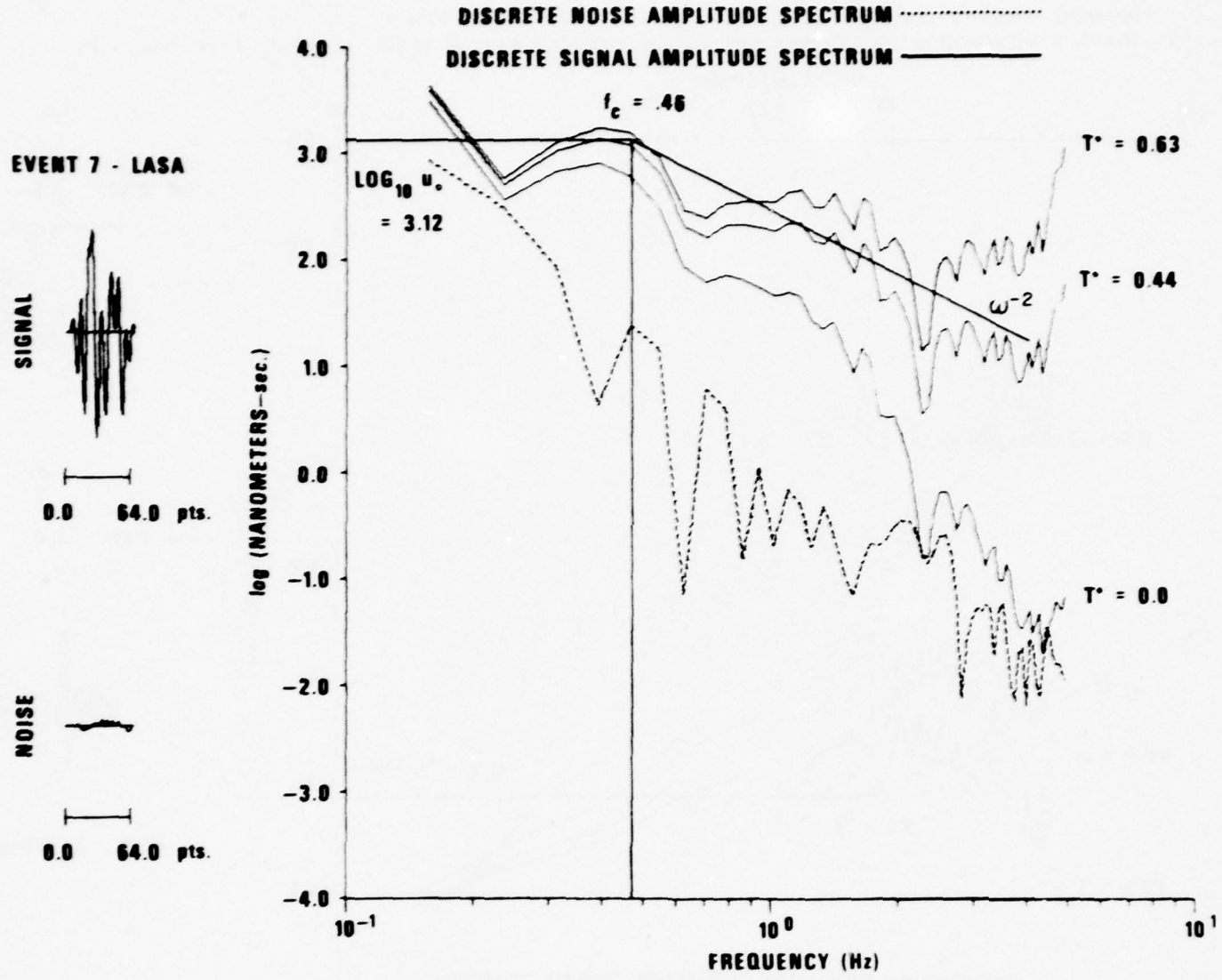

Figure 4 (cont.) LASA A0 and NORSAR C3 subarray spectra of P waves from Caucasus earthquakes with instrument response and attenuation removed.

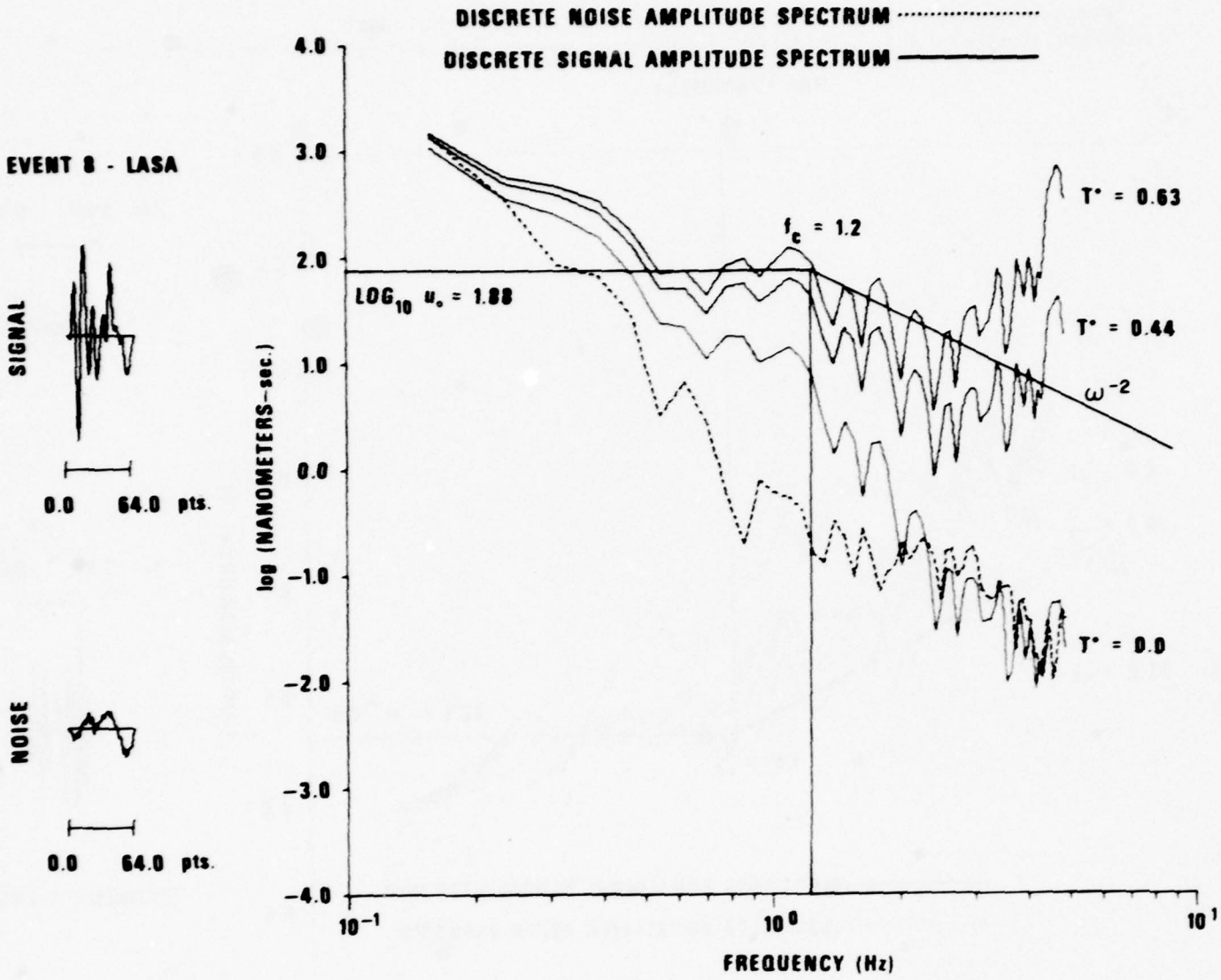

Figure 4 (cont.) LASA A0 and NORSAR C3 subarray spectra of P waves from Caucasus earthquakes with instrument response and attenuation removed.

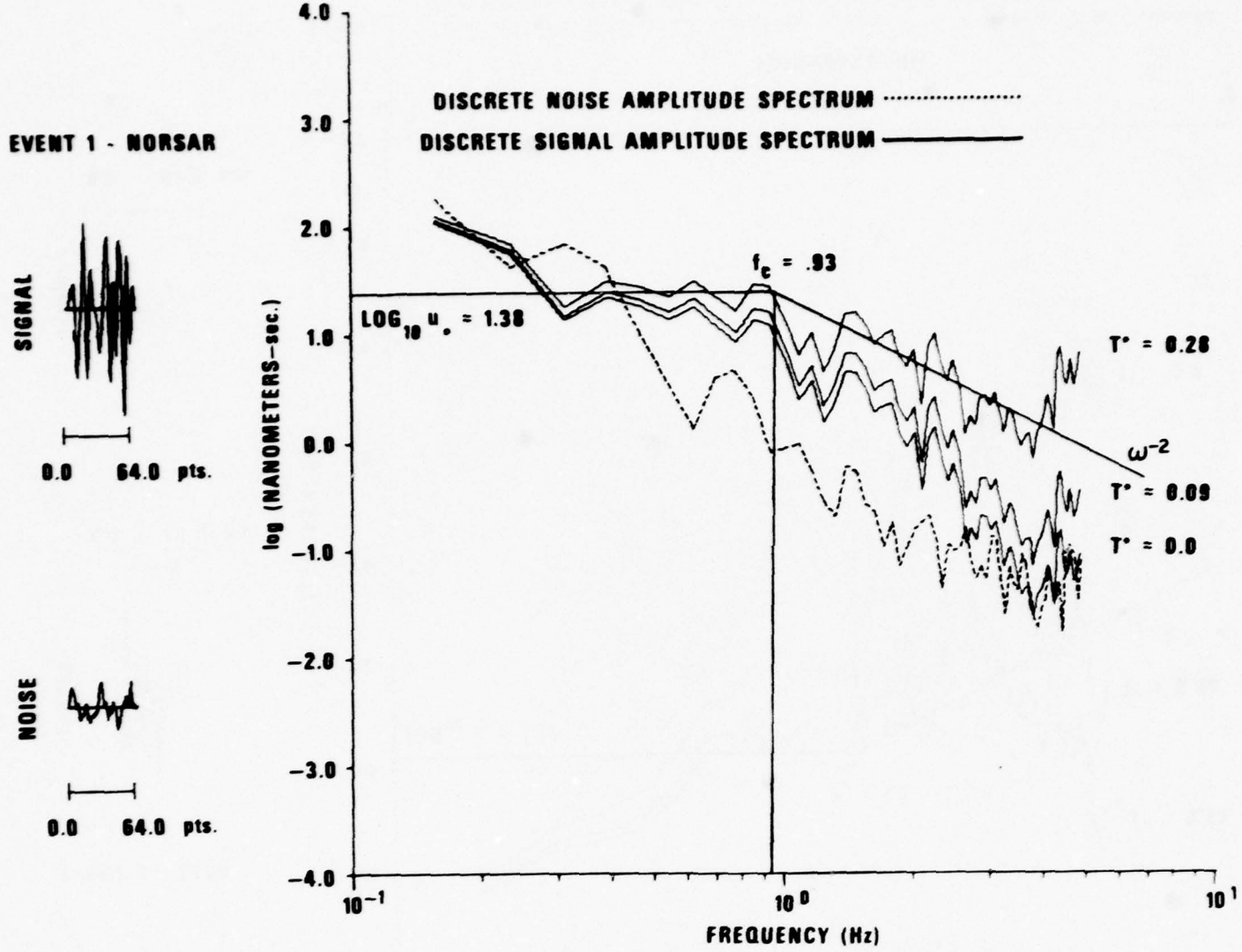

Figure 4 (cont.) LASA A0 and NORSAR C3 subarray spectra of P waves from Caucasus earthquakes with instrument response and attenuation removed.

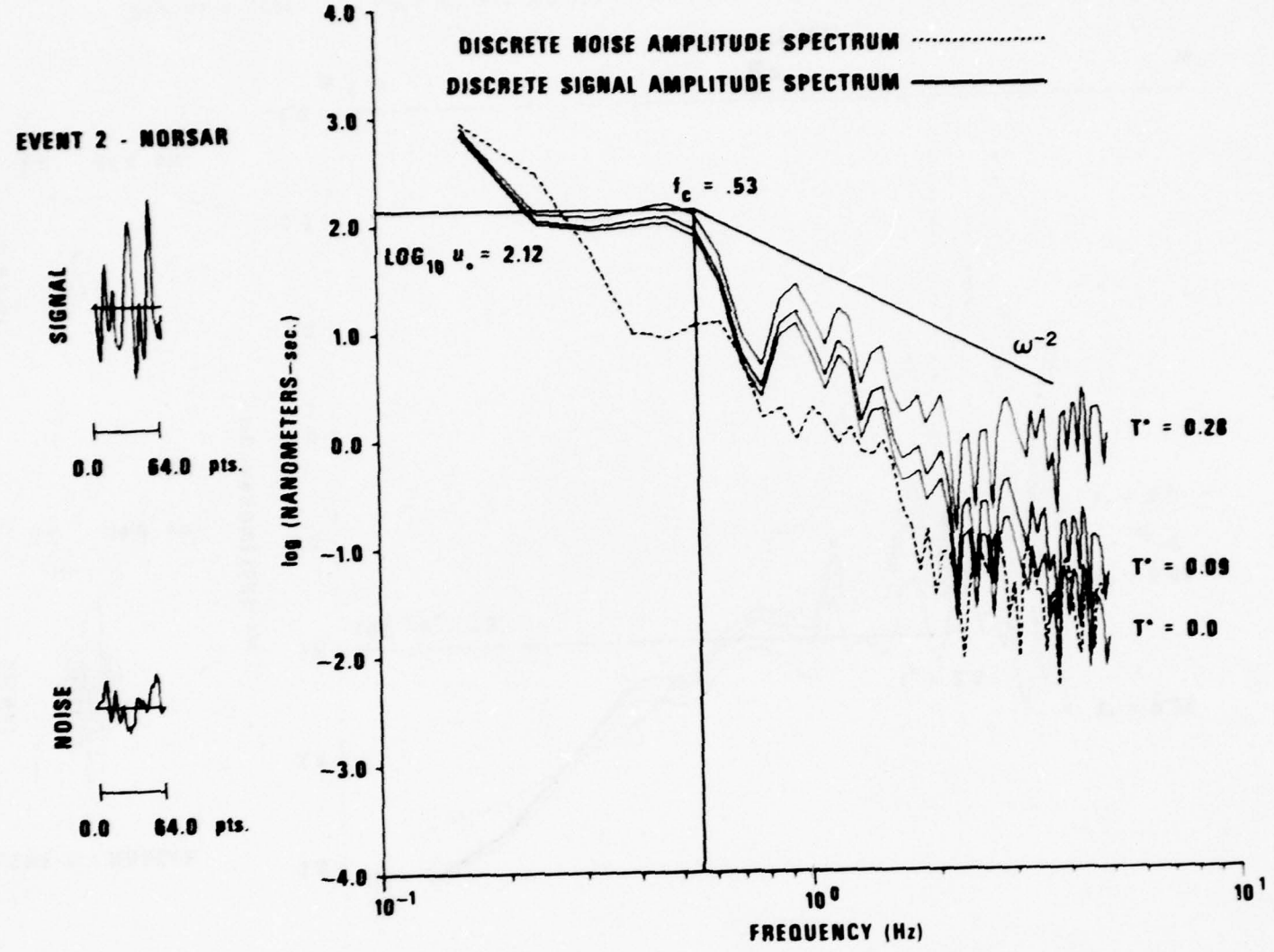

Figure 4 (cont.) LASA A0 and NORSAR C3 subarray spectra of P waves from Caucasus earthquakes with instrument response and attenuation removed.

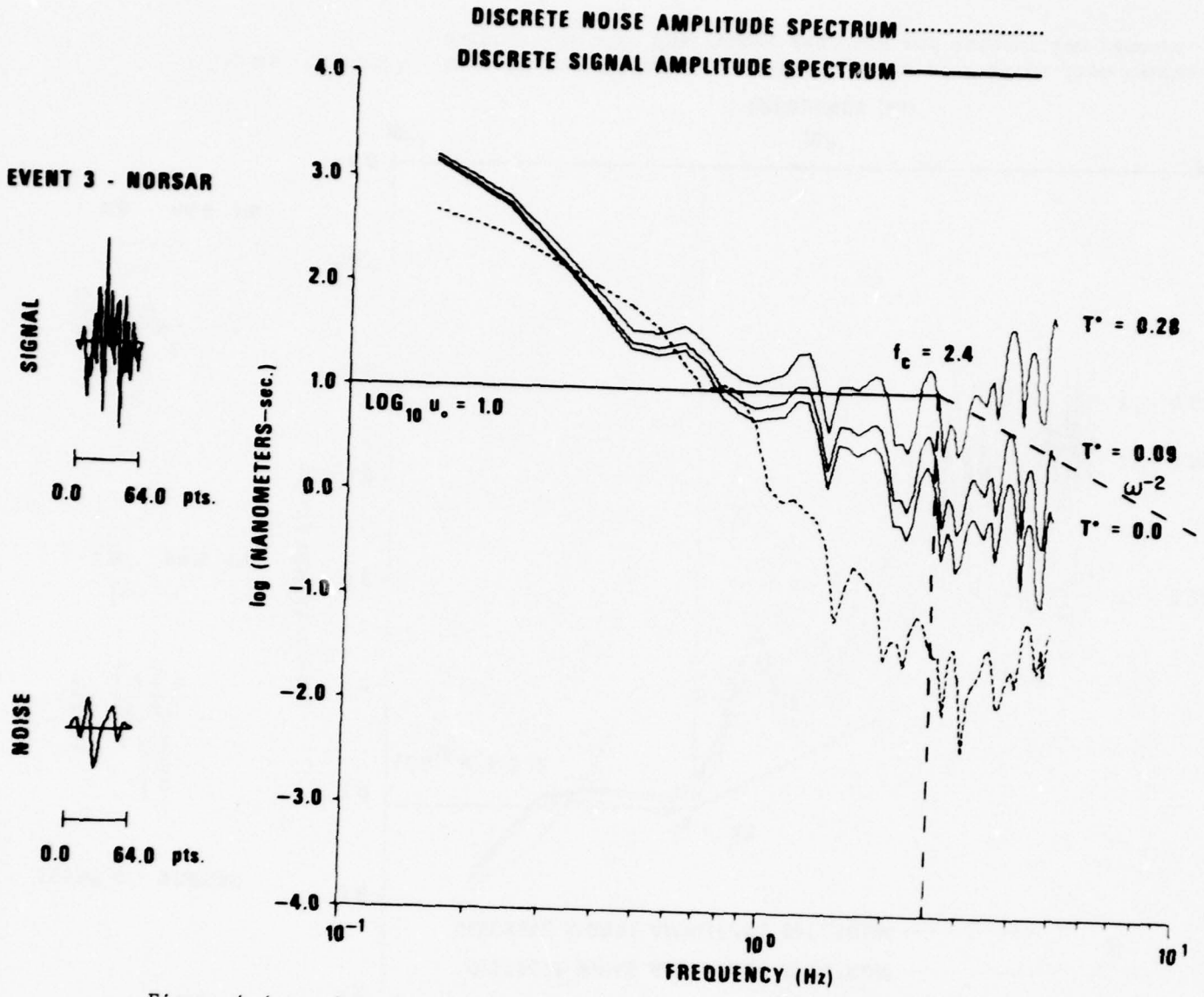

Figure 4 (cont.) LASA AO and NORSAR C3 subarray spectra of P waves from Caucasus earthquakes with instrument response and attenuation removed.

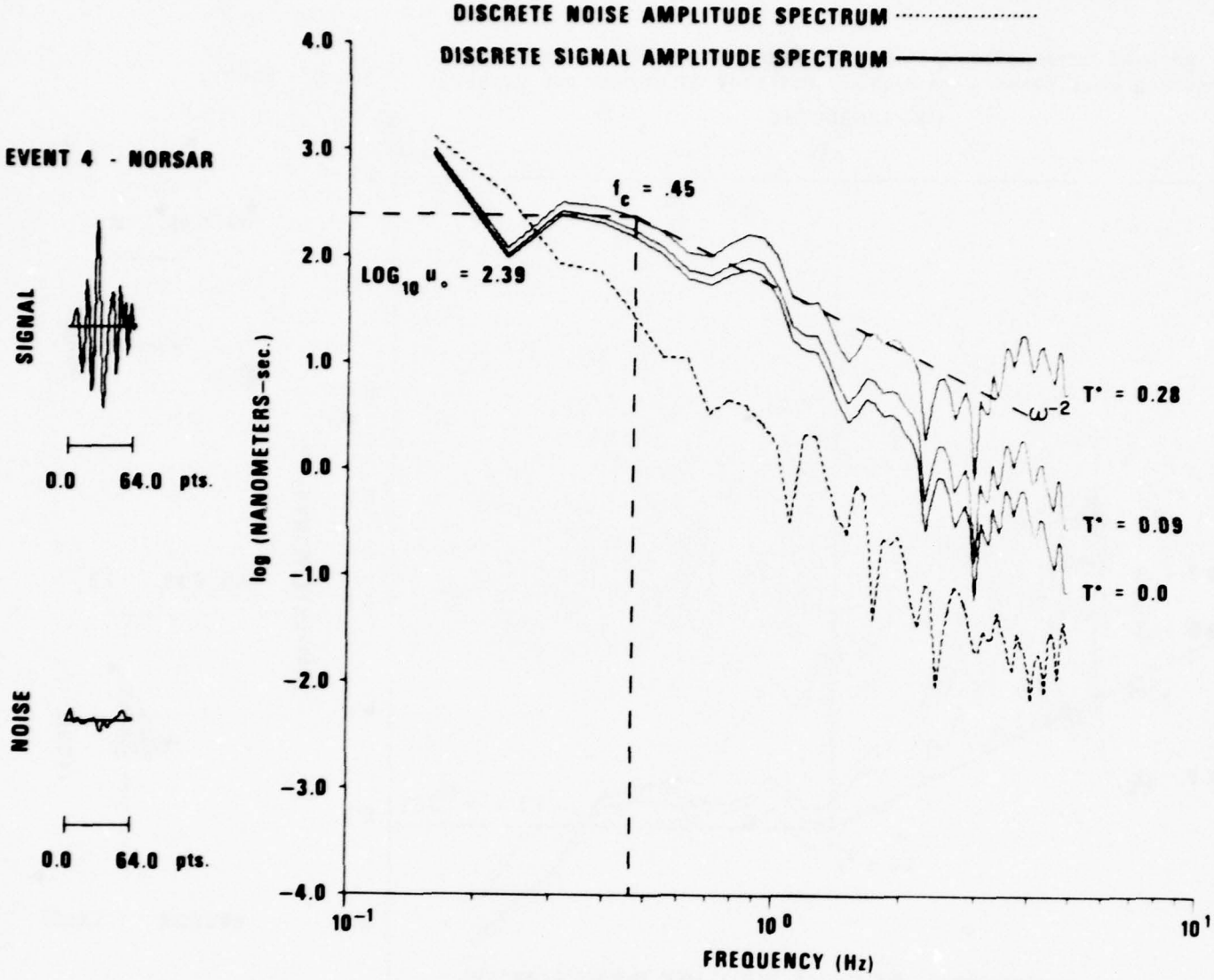

Figure 4 (cont.) LASA AO and NORSAR C3 subarray spectra of P waves from Caucasus earthquakes with instrument response and attenuation removed.

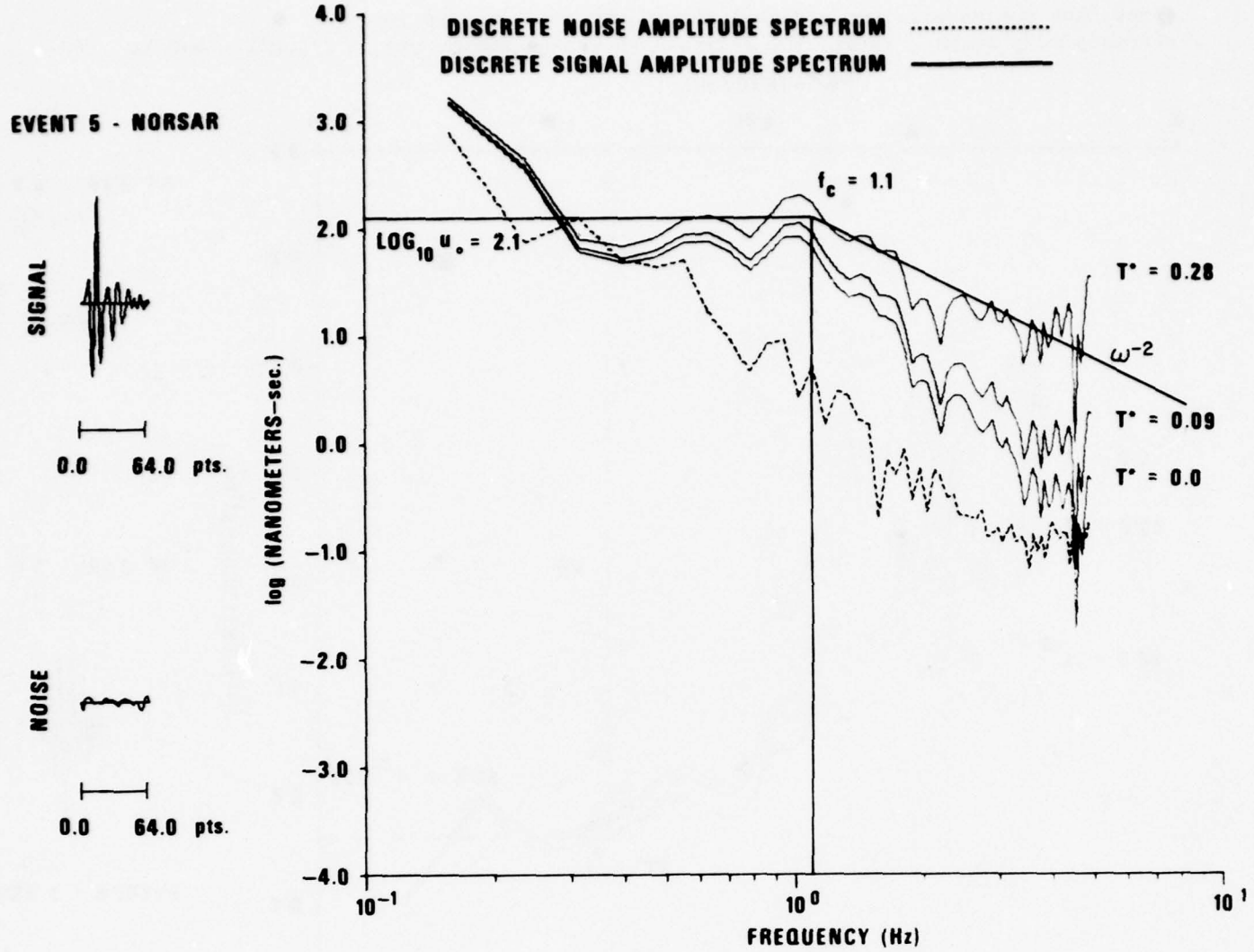

Figure 4 (cont.) LASA AO and NORSAR C3 subarray spectra of P waves from Caucasus earthquakes with instrument response and attenuation removed.

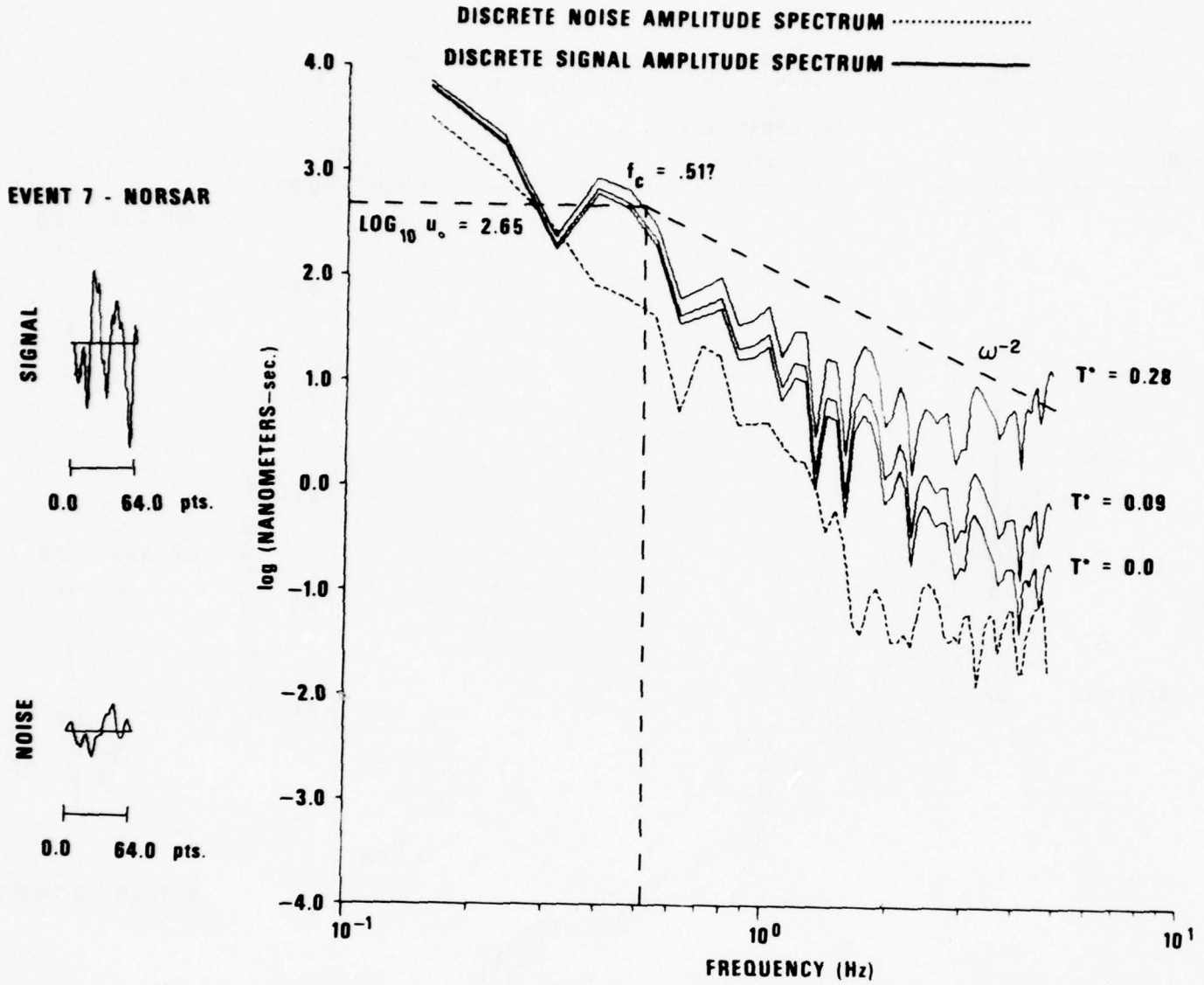

Figure 4 (cont.) LASA AO and NORSAR C3 subarray spectra of P waves from Caucasus earthquakes with instrument response and attenuation removed.

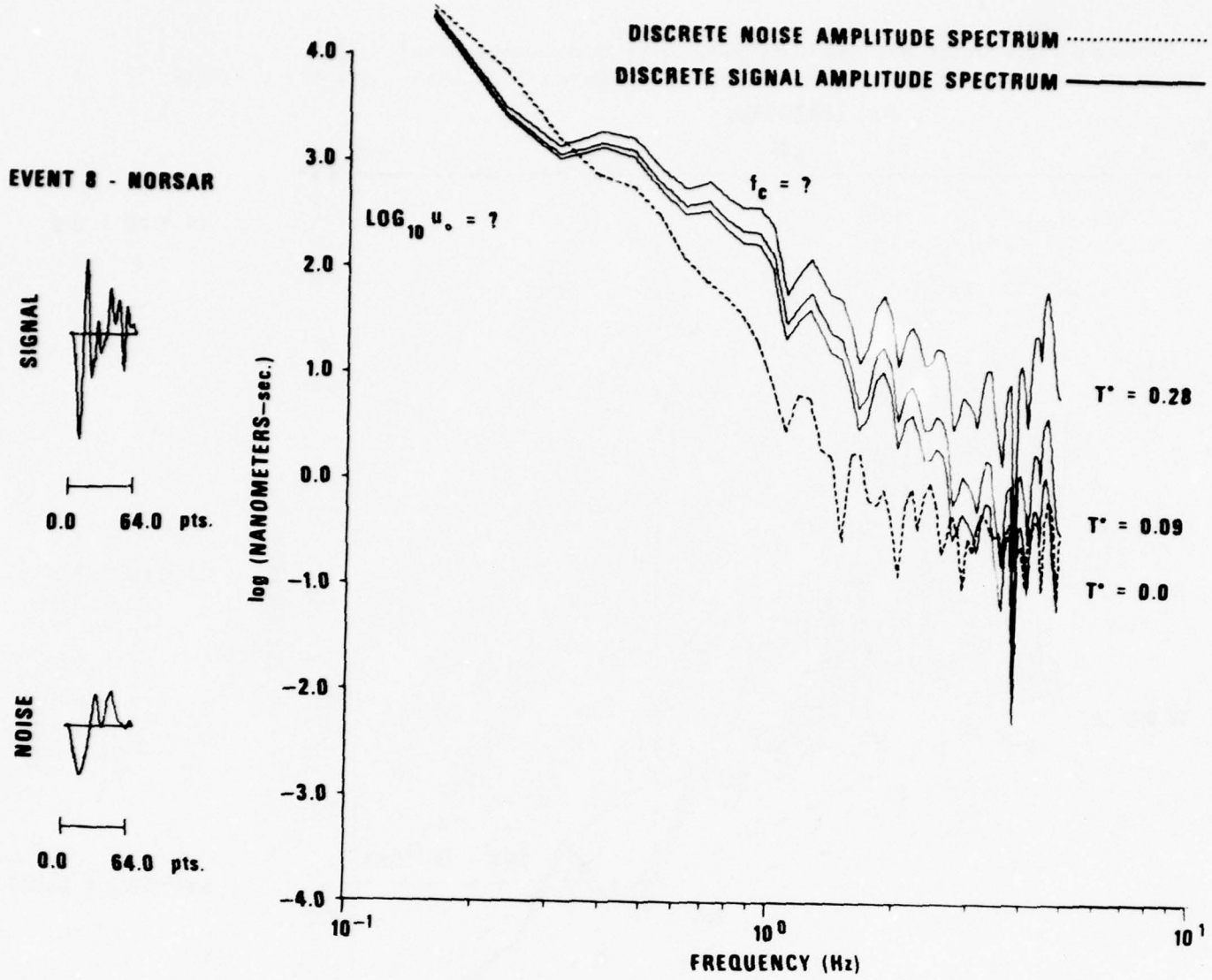

Figure 4 (cont.) LASA AO and NORSAR C3 subarray spectra of P waves from Caucasus earthquakes with instrument response and attenuation removed.

Seismic moment was calculated from the long-period body-wave spectral displacement $|\hat{u}_o|$ estimated in Figure 4 using the relation

$$M_o = \frac{4\pi\rho\alpha^3 D|\hat{u}_o|}{R_{\theta\phi}}$$

where $R_{\theta\phi}$ was assumed to be unity due to lack of knowledge of the focal mechanism, values of $\rho\alpha^3$ from Table I appropriate to the source depth were used, and the divergence factor D was applied (Ben-Menahem et al., 1965). A graph of moment versus corner frequency is shown in Figure 5. Our events fall close to or between the constant stress drop lines of Hanks and Thatcher (1972), indicating that our events are of intermediate stress drop.

We attempted to find the LR radiation pattern for each event by plotting the antilogs of the M_s values for each event as listed in Table IV. The results for the largest M_s earthquake, event 7, are shown in Figure 6. The maximum antilog is plotted on the outer circle, and all the other antilog values are scaled linearly between the center of the plot and the radius of the circle. The observed distribution of amplitudes does not obviously conform to any quadripole radiation pattern, which is probably due to varying propagation effects coupled with the large epicentral distances and the small magnitude of the events studied. The scatter of data points for all the events was so poor that no attempt was made to find the best-fitting radiation patterns.

Propagation Effects

We measured relative mantle attenuation along the paths from the Caucasus to LASA and NORSAR, the only two sites for which we had short-period digital data. Our measurement of attenuation is the factor t*, which is the travel time along the ray path divided by the average attenuation factor Q.

Ben-Menahem, A., S. Smith, and T. Teng, 1965. A procedure for source studies from spectrums of long-period seismic body waves, Bull. Seism. Soc. Amer., 55, 203.

Hanks, T., and W. Thatcher, 1972. A graphical representation of seismic source parameters, J. Geophys, Res., 77, 4393.

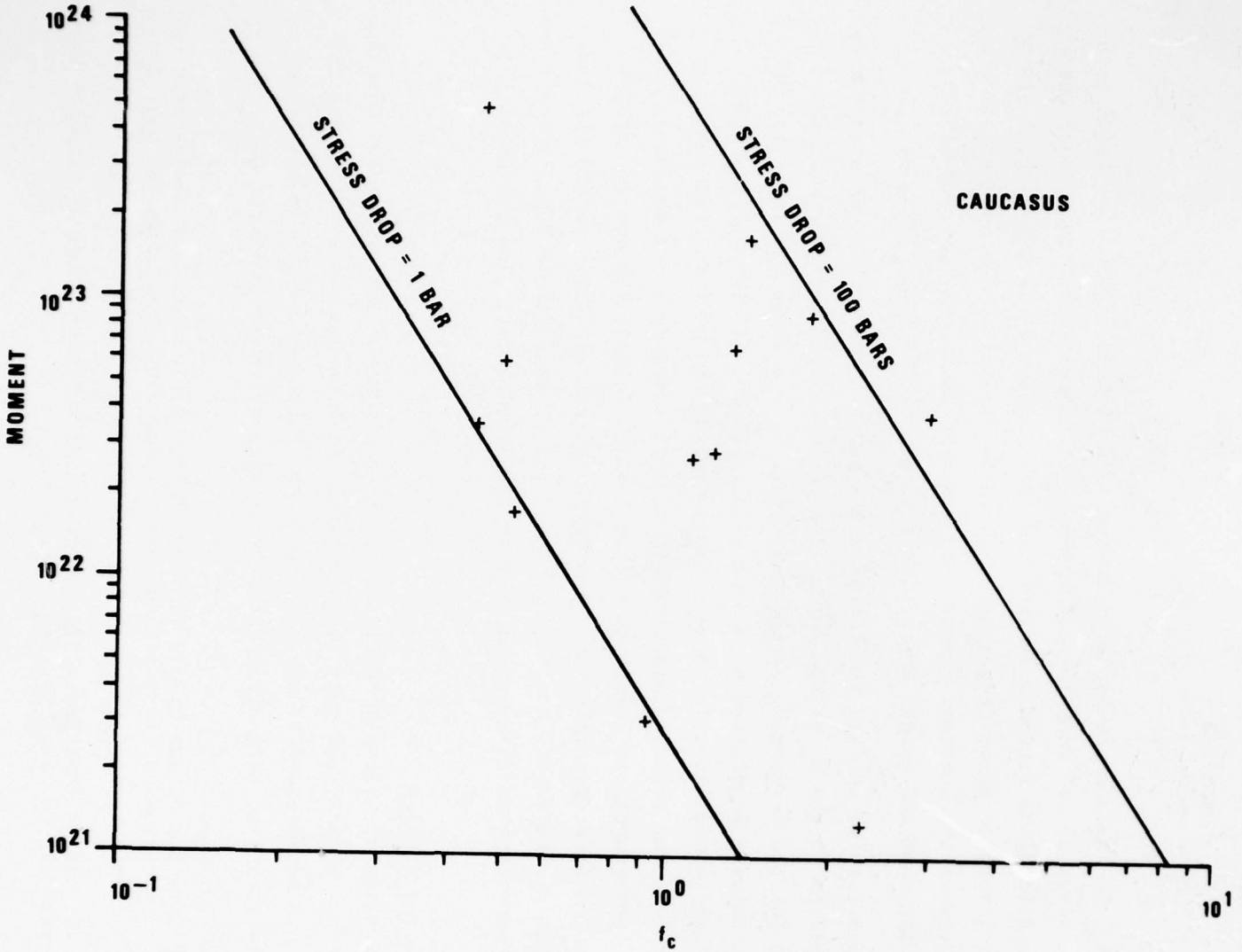

Figure 5. Seismic moment versus corner frequency for Caucasus earthquakes from LASA and NORSAR P recordings.

TABLE IV

Magnitude Data for Caucasus Earthquakes

Event 1

Station	Δ	m_b	M_s
BUL	64.0	4.76	
CHG	52.3		4.21
COL	72.3	4.44	
LASA	87.2	4.56	
MAT	69.4	5.50	
NAI	44.1	4.19	
NIL	25.0	4.56	
NORSAR	26.9	4.19	
NUR	21.3	4.10	
QUE	22.5	3.78	
SDB	63.5		4.68
SHL	43.0	4.16	
TOL	35.3	4.85	
AVERAGE		4.46	4.44

Event 2

Station	Δ	m_b	M_s
BAG	69.5	4.91	
BUL	62.8	4.97	
CHG	51.8	4.76	
COL	73.6	4.37	
EIL	13.6	4.29	
KOD	42.8	4.63	
KON	28.0	4.57	4.17
LASA	88.6		3.93
MAL	37.3		4.17
NIL	24.4	5.33	
NORSAR	28.2	4.88	3.62
NUR	22.7	4.53	
OGD	80.7	4.44	
POO	34.2	4.76	3.94
QUE	21.7	4.05	
SHL	42.5	4.56	3.79
TOL	35.9	4.70	3.84
AVERAGE		4.65	3.92

Event 3

Station	Δ	m_b	M_s
ALPA	73.0		3.67
BAG	65.8	5.00	
BUL	64.3	4.66	
CHG	48.3	4.99	3.66
COL	72.9	5.04	
EIL	16.2	3.80	2.96
FBK	73.0		3.88
GDH	55.7	5.25	
KOD	40.2	4.42	
KON	30.0	4.72	3.79
LASA	89.4	5.28	3.51
MAL	40.8	4.84	
MAT	66.5	4.84	4.83
NIL	21.0	5.12	
NORSAR	30.0	4.75	3.58
NUR	24.0	4.87	
OGD	82.8		4.45
POO	31.4	4.58	
QUE	18.6	3.93	3.42
SHL	38.9	4.91	3.63
TLO	39.3		3.09
AVERAGE		4.76	3.71

Event 4

Station	Δ	m_b	M_s
ALPA	73.7		4.67
ALQ	100.9		5.22
ALQ	100.9		5.43
BAG	66.0	5.00	4.54
BUL	63.6	4.96	
CHG	48.2		4.46
CHG	48.2		4.60
COL	73.6	5.31	4.94
CTA	108.7		5.22
EIL	15.6	4.47	
FBK	74.0		4.60
KON	30.5		4.11
KON	30.5		5.09
LASA	90.1	5.67	4.57
MAT	67.0		5.38
NAI	43.3	4.68	4.70
NIL	20.9	4.79	
NOR	46.2		4.58
NORSAR	30.5	5.29	
NUR	24.6	5.22	5.00
OGD	83.3		5.03
QUE	18.3	4.28	4.45
SDB	64.3	4.84	4.99
SHL	38.9		4.47
TOL	39.4	4.88	4.29
AVERAGE		4.93	4.77

Event 5

Station	Δ	m_b	M_s
ALPA	72.5		3.83
ALQ	100.0	4.46	
BAG	65.5	5.26	
BUL	64.8	4.80	
CHG	48.0	4.80	
COL	72.4	5.16	
CTA	108.5		4.00
DAG	44.4	5.09	
KOD	40.3	4.10	
KON	29.9		3.83
LASA	89.1	5.56	3.90
MAT	66.0		4.25
NAI	44.5		4.00
NIL	20.7	4.94	
NORSAR	29.9	5.49	3.38
NUR	23.8	5.27	
QUE	18.5	4.01	
SDB	65.5	4.96	
SHL	38.7	4.51	
TLO	39.6		3.72
AVERAGE		4.89	3.86

Event 6

Station	Δ	m_b	M_s
ALQ	98.3	4.60	4.77
BAG	66.9	5.00	4.55
BUL	65.5	5.06	4.61
CHG	49.7	4.97	4.24
CHG	49.7		4.48
CTA	110.1		4.53
DAG	42.8	4.60	
DAV	76.8		4.87
KIP	111.4		4.71
MAL	39.4	4.80	4.59
MAT	66.7	4.96	4.97
MAT	66.7		5.10
NAI	45.3	4.87	4.44
NIL	22.5	4.79	
NUR	22.0	5.23	
OGD	80.8		4.70
QUE	20.5		3.79
SDB	65.6	4.57	
TLO	37.8		4.14
AVERAGE		4.86	4.57

Event 7

Station	Δ	m_b	M_s
ALPA	71.6		4.78
ALQ	98.5	5.07	4.88
ALQ	98.5		4.82
BAG	67.0	5.54	4.85
BUL	65.3	5.00	4.83
CHG	49.7	5.30	
COL	71.6	5.03	4.99
CTA	110.1		4.61
DAG	43.0	4.70	
GDH	53.9	5.09	
LASA	87.7	5.89	
MAL	39.4	4.76	4.28
MAT	66.9		5.57
MAT	66.9		5.42
NAI	45.1	5.01	4.76
NIL	22.5	5.29	4.61
NORSAR	28.1	5.01	4.70
NUR	22.2	5.22	
QUE	20.4		4.01
SDB	65.4	4.96	5.31
TLO	37.8		4.14
AVERAGE		5.13	4.78

Event 8

Station	Δ	m_b	M_s
ALPA	72.2		3.69
ALQ	98.4	4.60	4.62
BUL	64.4	4.36	
CHG	50.9	4.54	3.39
COL	72.2	4.73	
DAG	43.0	4.80	
GDH	53.8	4.91	
KIP	112.6		4.58
LASA	87.7	5.19	4.01
MAT	68.2		4.25
NIL	23.6	4.50	
NORSAR	27.7	4.49	
NUR	21.9	4.79	
OGD	80.4	4.74	4.07
QUE	21.3	4.67	3.59
SDB	64.3	4.70	
SHL	41.6	4.33	3.68
TLO	36.7		3.78
AVERAGE		4.67	3.97

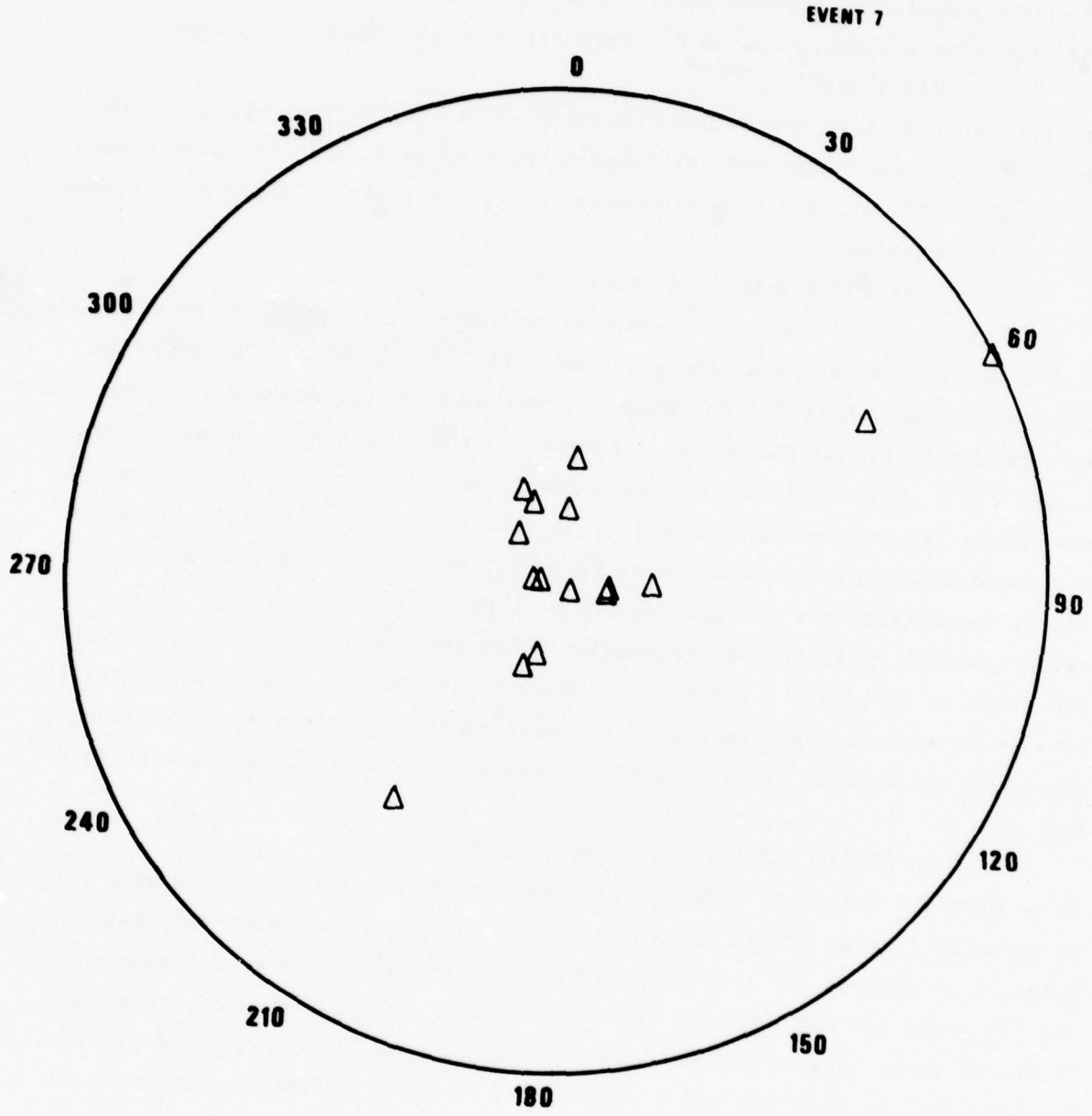

Figure 6. Observed LR amplitudes (T = 20 sec) for Caucasus event 7.

We determine t* by first normalizing and then summing the spectra shown in Figure 4 for each of the two paths - Caucasus to LASA and Caucasus to NORSAR. These averages are shown in Figure 7 and 8 and represent the average relative ground displacement density spectra at the true sites. If we assume that the source spectra has an f^{-2} fall off at high frequencies, then

$$F(f) \simeq S \cdot f^{-2} \cdot e^{-\pi f t^*}$$

for frequenceis above the corner frequency where F(f) is the average of the observed spectrum (corrected for seismograph response), S is the source spectrum scale constant, and f is frequency in Hz. Then after taking the natural log of this equation

$$\ell n\,[F(f)] + 2 \cdot \ell n(f) = -\pi t^* f + \ell n(S)$$

If we plot $\ell n\,[F(f)] + 2 \cdot \ell n(f)$ versus frequency for each path, as shown in Figures 9 and 11, the slope of the graph is $-\pi t^*$. We calculated the slope in the frequency range 1.0 to 2.5 Hz, where the signal to noise ratio was highest, and presumably beyond the corner frequency so that the high-frequency asyptotic slope of f^{-2} characterizes the source spectrum. Figure 5 shows that some of the corner frequencies are above 1 Hz, so the data may not be well fitted by the above equation; but if a higher frequency range were used, we would seriously contaminate the average spectra with background noise. The effect of using spectral estimates at frequencies below the corner frequency is to bias the slope or t* toward a lower value than the actual one. Thus our t* results here are not as reliable as needed to confidently quantify the attenuation along the two paths. Similarly, the equation for a source spectra with an f^{-3} fall off is

$$\ell n\,[F(f)] + 3 \cdot \ell n(f) = -\pi t^* f + \ell n(S)$$

If we plot the left hand side of this relation versus frequency for each path as shown in Figures 10 and 12, the slope of the graph is again $-\pi t^*$; but it is based on an assumed f^{-3} source spectrum. The t* values for an f^{-2} source model are .63 $\pm$ .08 for the Caucasus to LASA path and .28 $\pm$ .06 for the Caucasus to NORSAR path. The t* values for an f^{-3} source model are .44 $\pm$ .08 for the Caucasus to LASA path and .09 $\pm$ .05 for the Caucasus to NORSAR path. We add that there is a predominance of theoretical models which imply a f^{-2} source spectrum rather than a f^{-3} one (Geller, 1976).

Geller, R. J., 1976. Scaling relations for earthquake source parameters and magnitude, Bull. Seism. Soc. Am., 66, 1501.

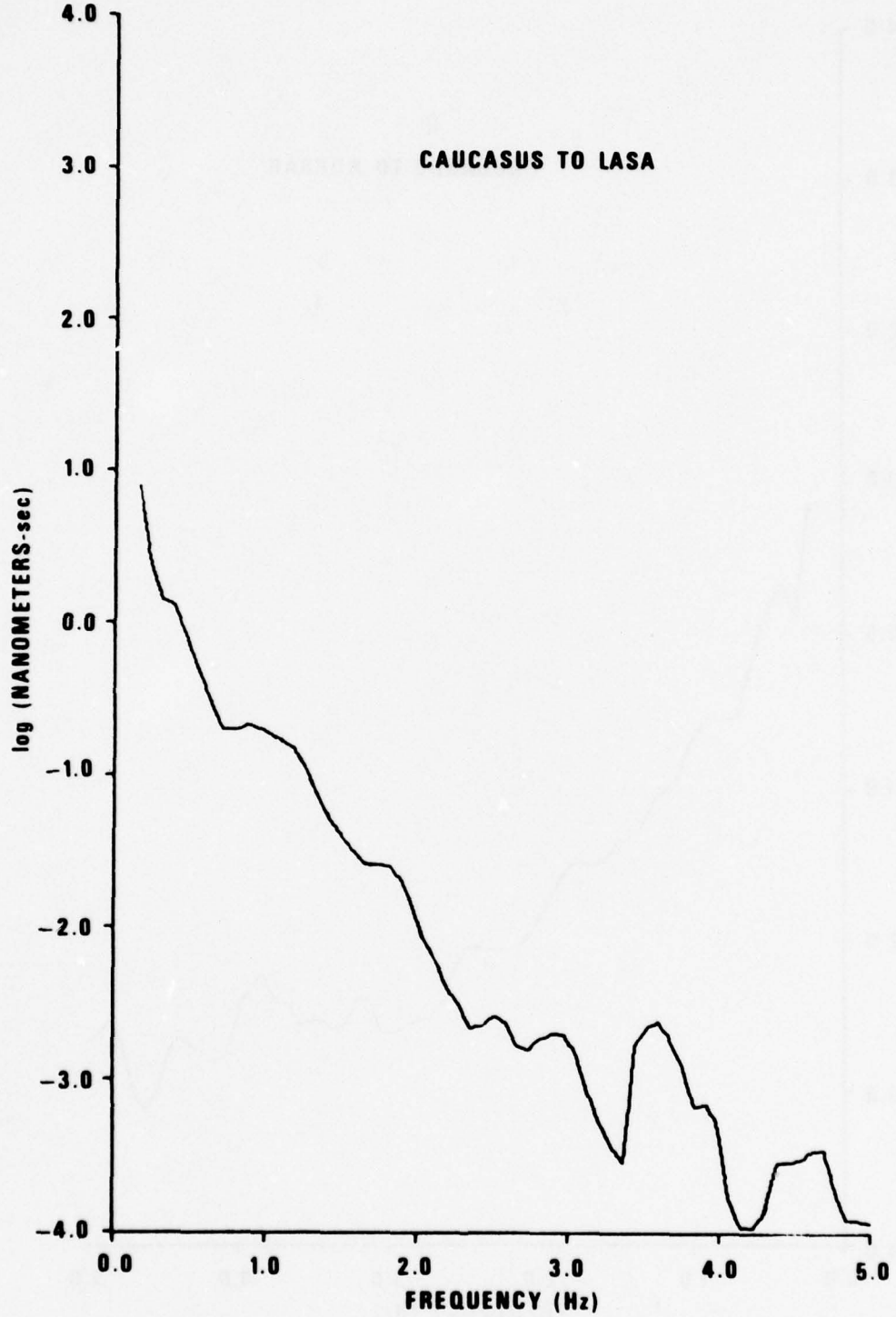

Figure 7. Average of all short-period P spectra for the path Caucasus to LASA.

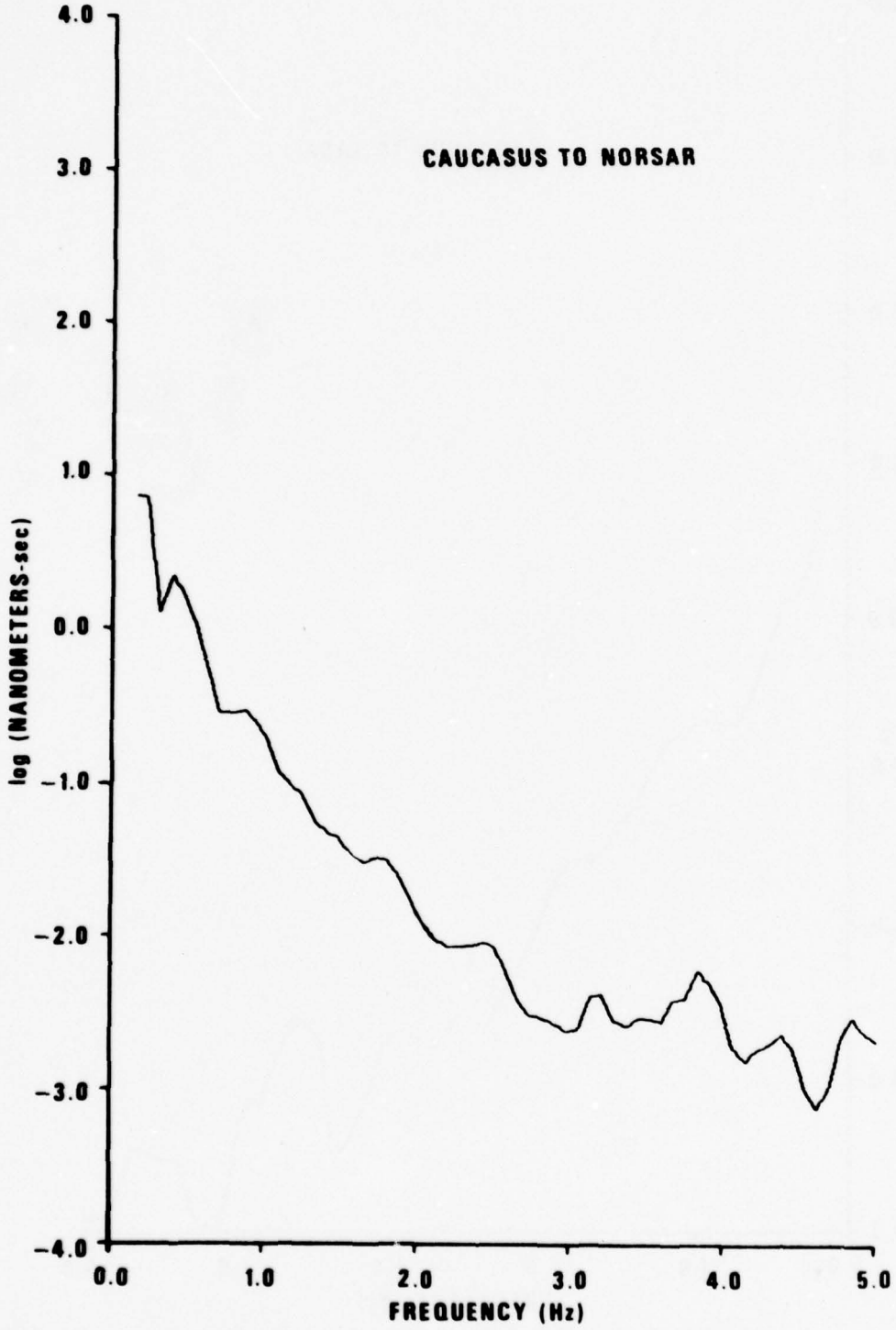

Figure 8. Average of all short-period P spectra for the path Caucasus to NORSAR.

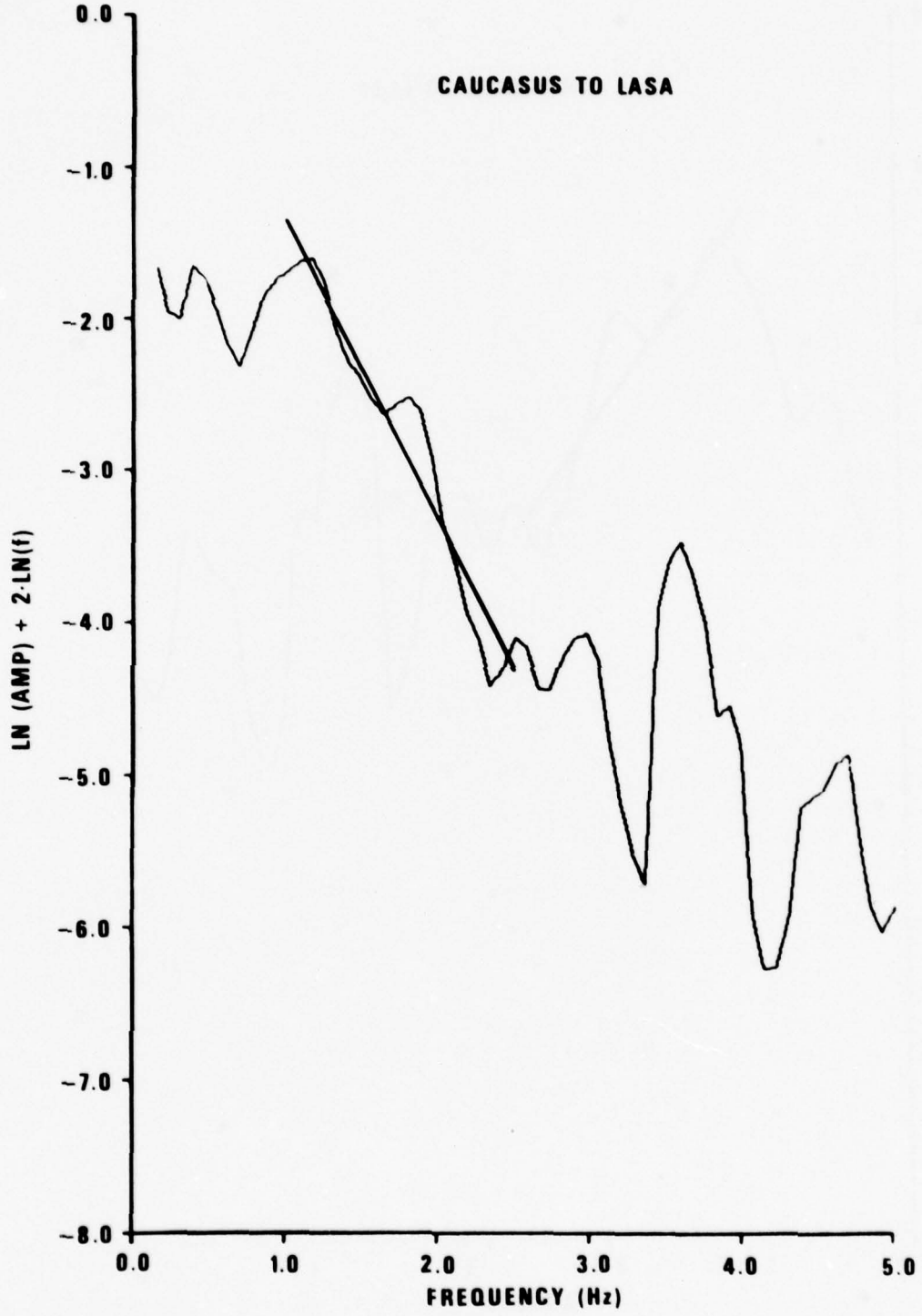

Figure 9. Ln(F) + 2·ln(f) versus frequency for the path Caucasus to LASA.

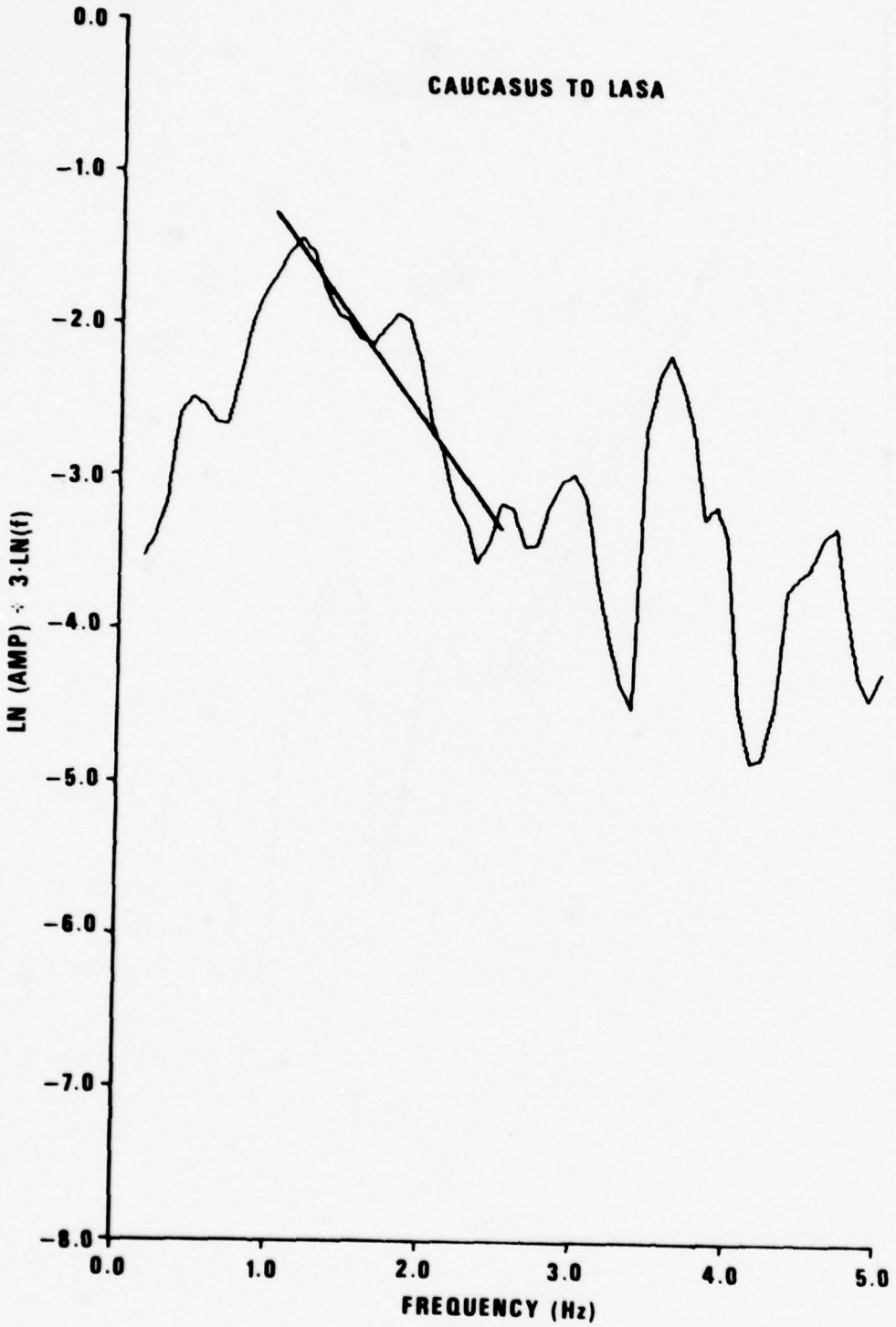

Figure 10. Ln(F) + 3·ln(f) versus frequency for the path Caucasus to LASA.

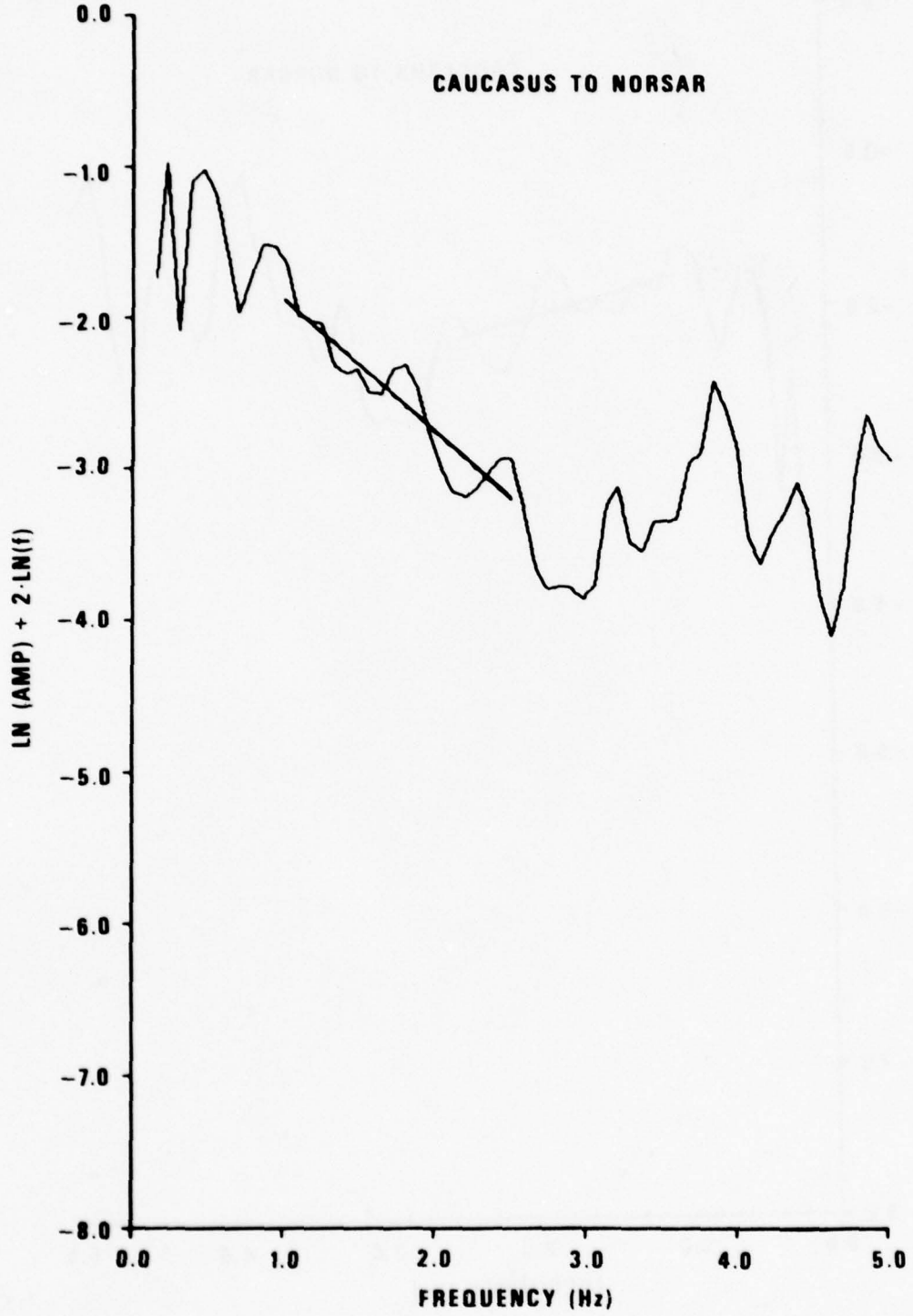

Figure 11. Ln(F) + 2·ln(f) versus frequency for the path Caucasus to NORSAR.

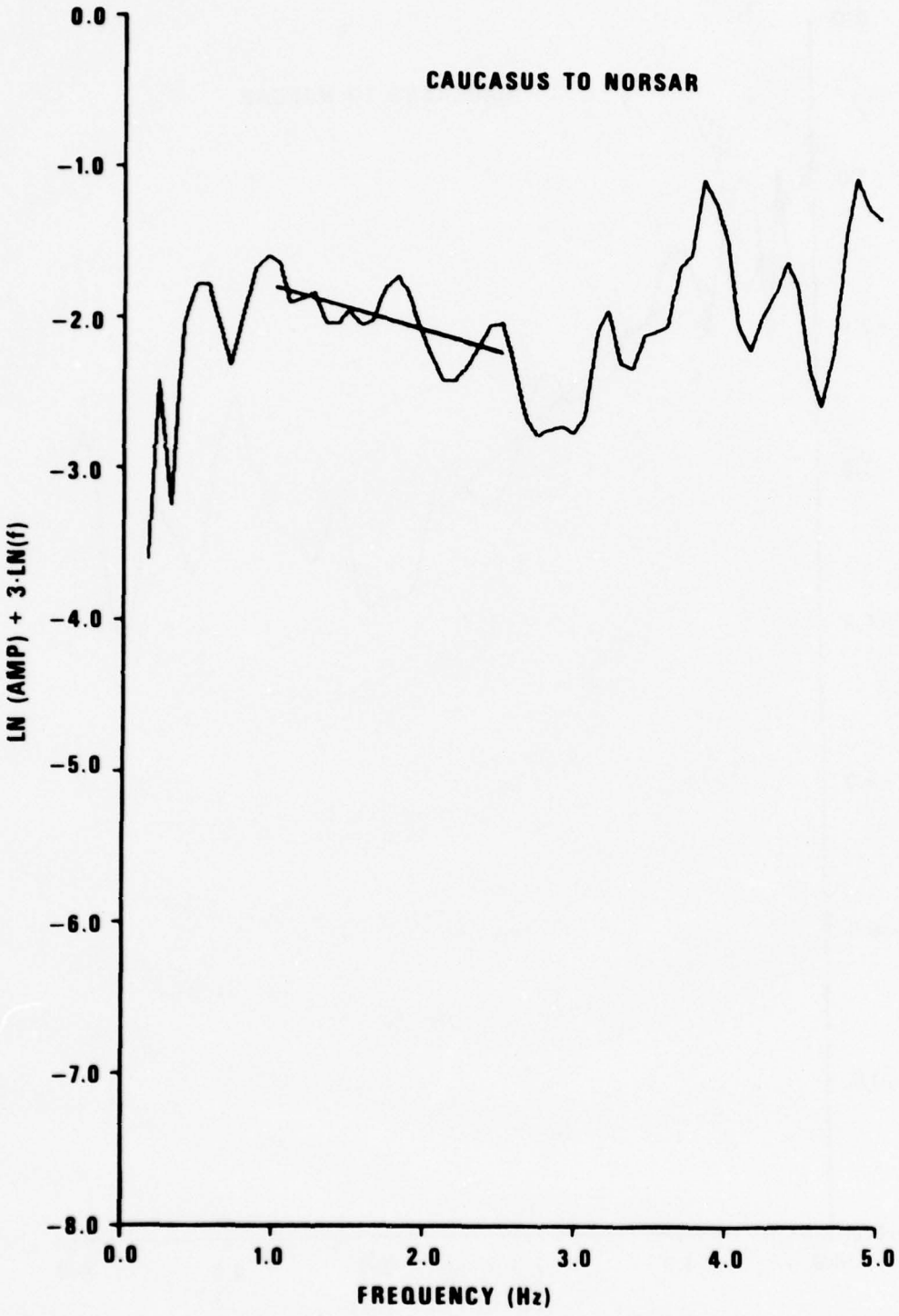

Figure 12. Ln(F) + 3·ln(f) versus frequency for the path Caucasus to NORSAR.

There appears to be is a real difference in attenuation between the two paths as revealed in the spectra; note that the waveforms in Figure 2 do not clearly reflect this. The Caucasus to NORSAR path has less attenuation, as expected since the path is mostly through continental shield areas. Values of t* for the explosions for an f^{-2} source model were also calculated (von Seggern and Blandford, 1972). These t* values are .35 $\pm$ .17 for the southwest USSR (events 1 and 2) to LASA path, .29 $\pm$ .13 for the West Kazakh (events 3 through 6) to LASA path, .19 $\pm$ .04 for the West Kazakh to NORSAR path, .16 $\pm$ .10 for the East Kazakh (events 7 and 8) to LASA path and .05 $\pm$ .08 for the East Kazakh to NORSAR path. NORSAR signals were not recovered for the southwest USSR explosions. As expected, the explosion t* values for the paths to NORSAR are lower than the values for the paths to LASA since the path to NORSAR is through continental shield areas while that to LASA passes through the more complicated tectonic province of the western United States, where attenuation is known to be high.

von Seggern and Sobel (1975) have presented a method of predicting 20-second Rayleigh-wave amplitudes by geometrical ray tracing. Their work shows that lateral changes in 20-second LR-phase velocity can cause major multipathing and also large teleseismic amplitude variations due to accumulated small-scale refraction effects. Figure 13 illustrates the paths of rays which result for event 7 (42.9N, 47.0E). (The rays which pass close to the North Pole were stopped close to that point due to ray-tracing numerical problems near the poles.) No attempt is made to quantitively relate these patterns to observed LR amplitudes since we cannot correct the predicted amplitude for source mechanism, but we can qualitatively compare the pattern of rays to M_s residuals calculated from the magnitude data in Table IV. Where the rays cross we can expect either constructive interference (large positive residuals as at ALQ, MAT, OGD and SDB in Table IV) or destructive interference (large negative residuals as at NORSAR, QUE and TOL). The M_s residuals at CHG and LASA are negative, as can be predicted from the diverging raypaths near those sites. Stations which record a stable amplitude are desirable for calibrating a source region in magnitude

---

von Seggern, D., and R. Blandford, 1972. Source time functions and spectra for underground nuclear explosions, Geophys, J., 31, 83-97.

von Seggern, D., and P. Sobel, 1975. Experiments in refining Ms estimates for seismic events, SDAC Report No: TR-75-17, Teledyne Geotech, Alexandria, Virginia.

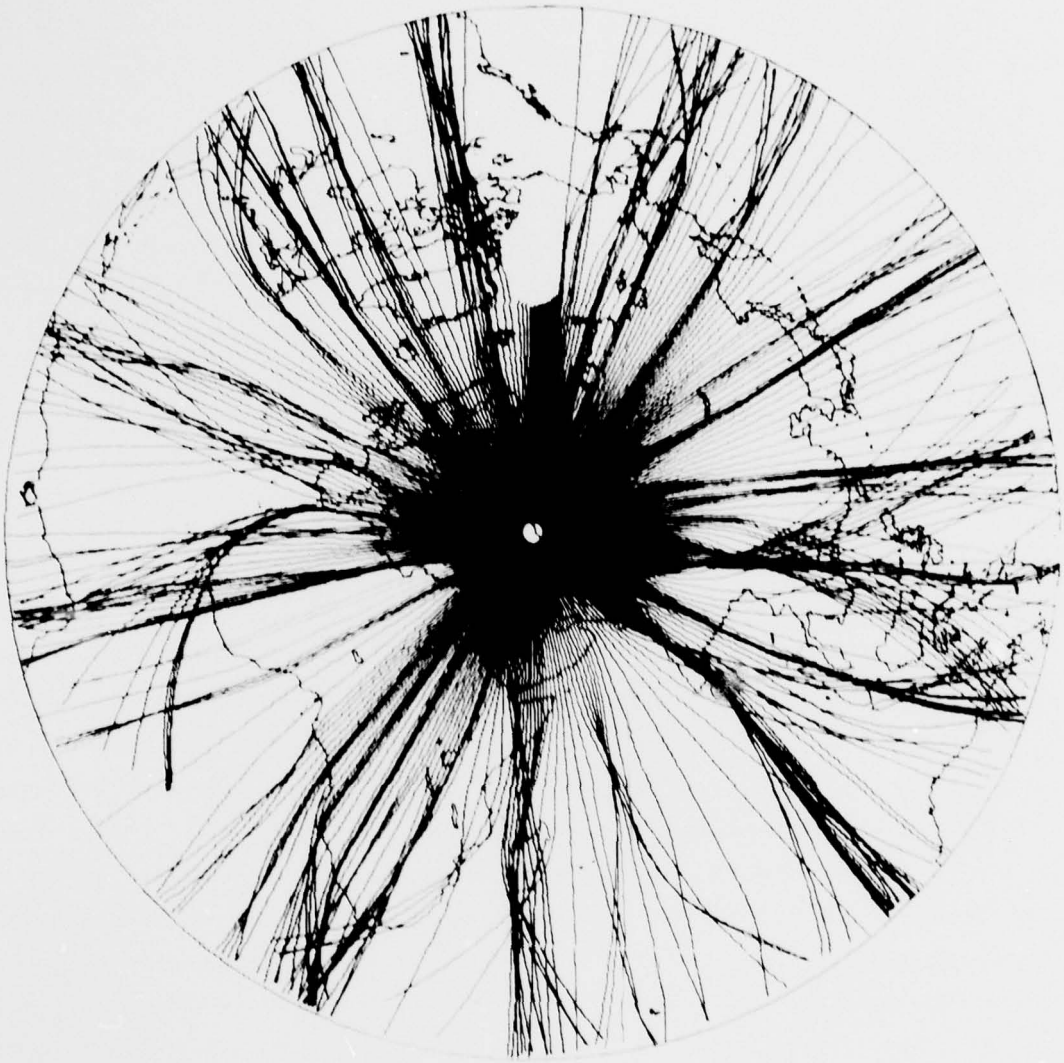

Figure 13. Predicted LR raypaths (T = 20 sec) for event 7 (42.9N, 47.0E).

determination. For events from the Caucasus, such stations could be located in eastern China and USSR and central Europe. The complicated LR ray-tracing figure partially explains why we were unable to determine LR radiation patterns from our amplitude observations.

DISCRIMINATION ASPECTS

M_s-m_b

In this and the following sections we apply several common discriminants between earthquakes and explosions to the Caucasus earthquakes and Kazakh and Southwest Russia explosions. We independently determined average M_s and m_b values for the Caucasus events in Table II using WWSSN stations, HGLP stations, and the ALPA, LASA, and NORSAR arrays. The data used in the average estimates is listed in Table IV. Negative values in the table indicate noise measurements which were used as upper bounds for the signal amplitudes. Magnitudes were computed according to the formulas

$$m_b = \log (A/T) + B(\Delta)$$

$$M_s = \log (A/T) + 1.66 \log \Delta + 0.3$$

where A = one-half the peak-to-peak maximum recorded amplitude reduced to mμ ground displacement,

T = period in seconds (restricted to 17 to 23 sec for M_s calculations),

Δ = epicentral distance in degrees,

$B(\Delta)$ = Gutenberg-Richter correction term for surface-focus P waves.

We also independently determined M_s for the Kazakh and Southwest USSR explosions in Table III using the NORSAR array and HGLP stations. The data used in the average estimates for explosion M_s are listed in Table V, and explosion m_b values are from the NEIS list. Throughout we have used a method of magnitude averaging proposed by Ringdal (1976) in which the magnitudes at the individual stations are assumed to follow a Gaussian distribution. Among this distribution, amplitudes corresponding to some magnitudes will fall below the noise level; and Ringdal's method then substitutes a noise measurement at those stations which don't detect and computes the maximum likelihood estimate of magnitude based on measured signals and noise. The effect of this procedure is to more accurately define the magnitude of events not widely recorded; more specifically, it usually results in a lower magnitude than that produced by routine averaging of observed magnitudes. The M_s-m_b plot using this method for all the events of this study is shown in Figure 14. Note that two explosions (events 7 and 8 in East Kazakh) had no LR detections, and an upper bound has been plotted for M_s using the NORSAR noise level of Table V.

Ringdal, F., 1976, Maximum-likelihood estimate of event magnitude, Bull. Seism. Soc. Am., 66, 789.

TABLE V

Magnitude Data for Kazakh and southwest USSR Explosions

Event 1

Station	Δ	M_s
CHG	50.1	4.25
EIL	21.0	4.25
KON	25.2	4.25
NAO	35.9	4.92
AVERAGE		4.44

Event 2

Station	Δ	M_s
KON	24.3	3.25
NAO	25.4	3.55
AVERAGE		3.40

Event 3

Station	Δ	M_s
CHG	42.8	-3.44
KON	30.7	2.86
AVERAGE		2.86

Event 4

Station	Δ	M_s
CHG	35.8	-3.83
KON	38.4	3.67
MAT	53.3	-3.85
AVERAGE		3.60

Event 5

Station	Δ	M_s
KON	36.6	3.31
MAT	52.1	-4.08
AVERAGE		3.31

Event 6

Station	Δ	M_s
KON	26.0	3.54
AVERAGE		3.54

Event 7

Station	Δ	M_s
NAO	38.1	-2.61
AVERAGE		-2.61 (maximum)

Event 8

Station	Δ	M_s
NAO	38.9	-3.10
AVERAGE		-3.10 (maximum)

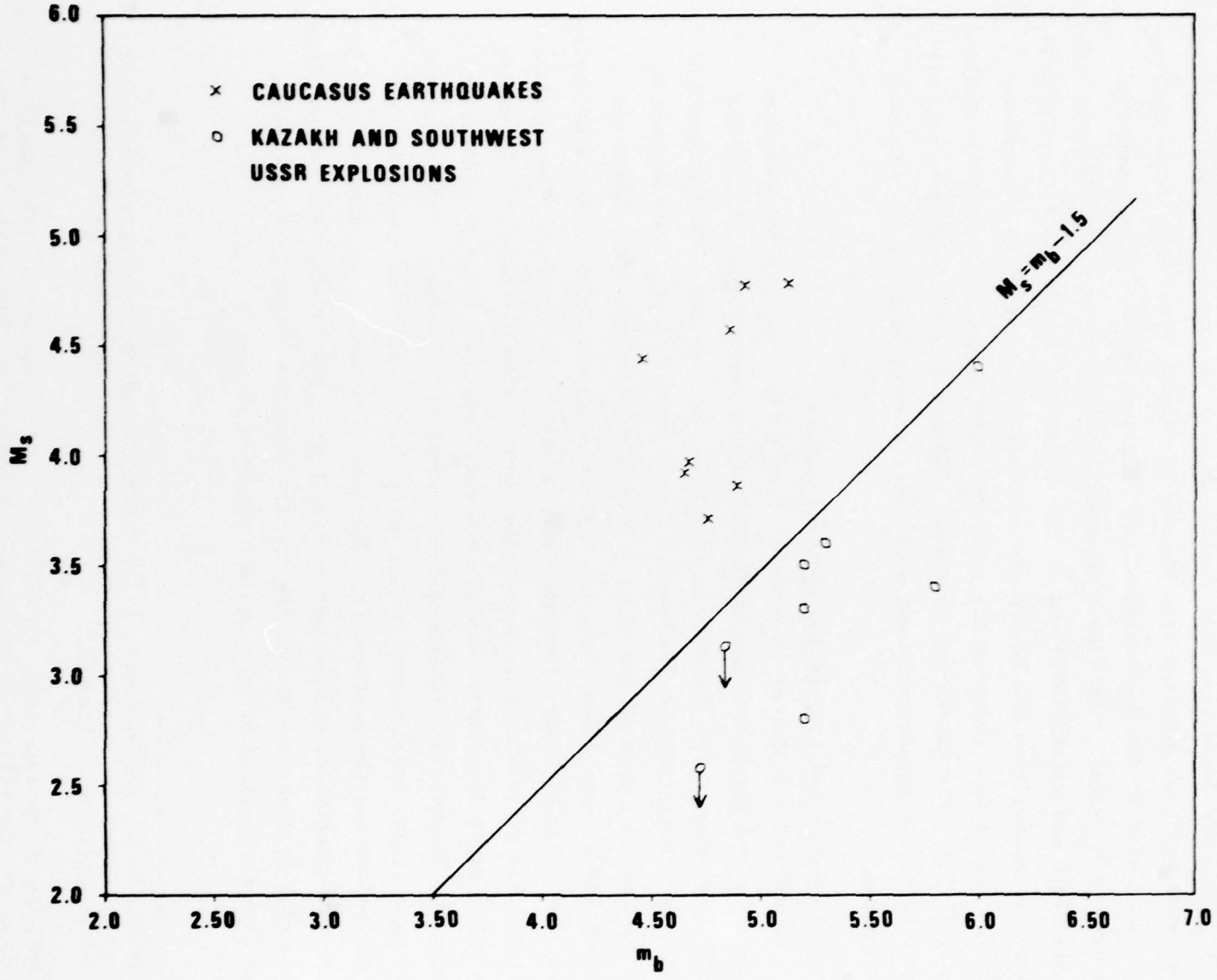

Figure 14. M_S vs. m_b for Caucasus earthquakes and Kazakh and southwest USSR explosions.

The magnitude averages of those events where many of the readings are noise levels are lower than what would result if only measured signal amplitudes were used, as expected from Ringdal's method. Where only noise measurements were used in the M_s determination, an arrow in the figure represents the maximum M_s value. The line $M_s = m_b - 1.5$ (suggested as a discriminant line by Blandford and Clark (1975) and earlier workers) clearly separates the Caucasus earthquakes from the Kazakh and southwest USSR explosion population. This line would also separate the suite of Asian events studied by the Dahlman et al. (1974). The Kazakh and southwest USSR explosions are located approximately 10 to 25 degrees north and northeast, respectively, of the Caucasus earthquakes.

Corner Frequency and Long-Period Spectral Level

Figure 15 is a plot of $|\Omega_o|$ versus corner frequency for the Caucasus earthquakes and Kazakh and southwest USSR explosions recorded at LASA and NORSAR. No long-period P phases were recorded at the long-period arrays due to the small magnitudes of the events, so the values of $|\Omega_o|$ were estimated from the spectral data of the short-period vertical component. Hanks and Thatcher (1972) have shown that, for a given long-period level, Amchitka explosions have a higher corner frequency than Aleutian earthquakes. The physical basis of this discriminant is the smaller source time dimension of the explosion for a given long-period level. However, Figure 15 shows no separation between the Caucasus earthquakes and the Kazakh and Southwest USSR explosions. There is a slight trend toward higher corner frequencies for lower $|\Omega_o|$ for the explosions and the earthquakes. The lack of a clear discriminant could be due to characteristics of the sources examined in this study. Another possible explanation is that, due to the low magnitude of the events studied here, a clear asymptotic value of $|\Omega_o|$ was not possible in most cases.

Blandford, R. R., and D. Clark, 1975, Variability of seismic waveforms recorded at LASA from small subregion of Kamchatka, SDAC-TR-75-12 Teledyne Geotech, Alexandria, Virginia.

Dahlman, O., I. H. Israelson, A. Austegard, and G. Hornstrom, 1974, Definition and identification of seismic events in the USSR, Bull. Seism. Soc, Am., 64, 607.

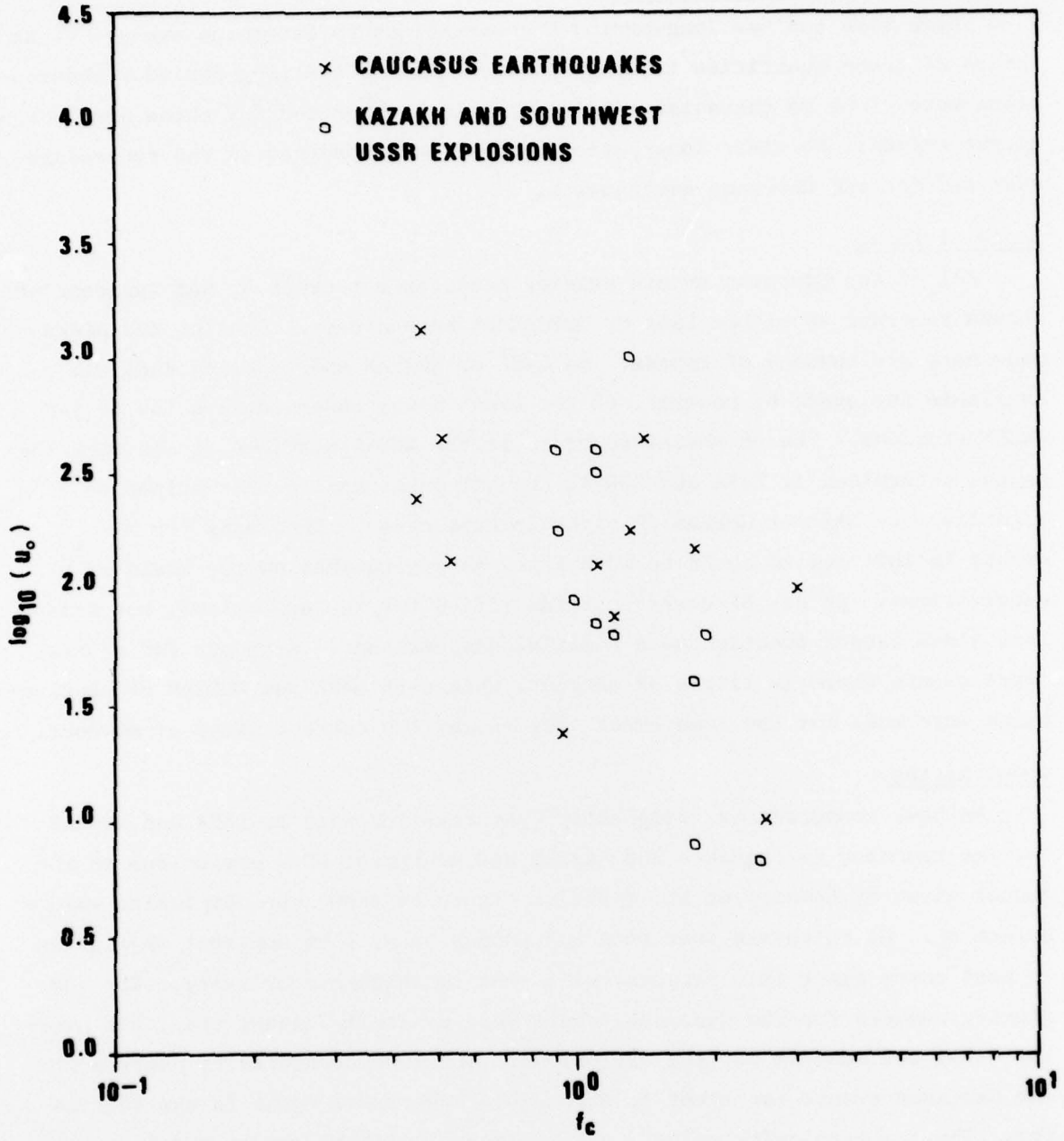

Figure 15. Long-period spectral level vs. corner frequency for Caucasus earthquakes and Kazakh and southwest USSR explosions from LASA and NORSAR P recordings.

Long-Period Body-wave Excitation

There were too few long-period P observations to determine average event ratios of these quantities to other phases. All of the long-period P observations were close to the noise level, as would be expected for these small-magnitude events. No clear long-period S waves were observed on the recordings analyzed for the Caucasus earthquakes.

Depth of Focus

All of the Caucasus events studied here, except event 6, had apparent pP phases recorded at either LASA or NORSAR or both arrays. Some of the picks made here are tenuous of course. No LASA or NORSAR short-period data was available for event 6; however, pP for event 6 was observed at a few of the WWSSN stations. The pP phases recorded at the WWSSN stations agreed with the depths determined at LASA and NORSAR for all cases and in fact helped to establish the LASA or NORSAR pP picks in some cases. Thus many low M_s-m_b events in this region could be identified as earthquakes on the basis of pP observations. pP was of course not identified for the explosions, but this fact alone cannot function as a positive discriminant. Although for crustal depth events there is little pP moveout, when both LASA and NORSAR pP observations were made for the same event they showed the correct sense of moveout.

Complexities

We have computed the "complexity" parameter as seen at LASA and NORSAR for the Caucasus earthquakes and Kazakh and southwest USSR explosions in the manner given by Lambert et al. (1969). Figure 16 shows the complexity values versus m_b. We reiterate that LASA and NORSAR beams show apparent pP signals in most cases since this presense will tend to enhance complexity. The complexity numbers for the Caucasus events were generally higher than, but overlap with, the numbers for the explosions. The lowest complexity numbers for the Caucasus events for event 5, a possible subcrustal event in the Caspian Sea. The low complexity value for this event is likely due to the late arrival of the pP signal, beyond the 30-sec signal window used.

Lambert, D., D. von Seggern, S. Alexander, and G. Galat, 1969. The LONGSHOT Experiment, Volume II. Comprehensive Analysis, SDL Report No. 234, Teledyne Geotech, Alexandria, Virginia.

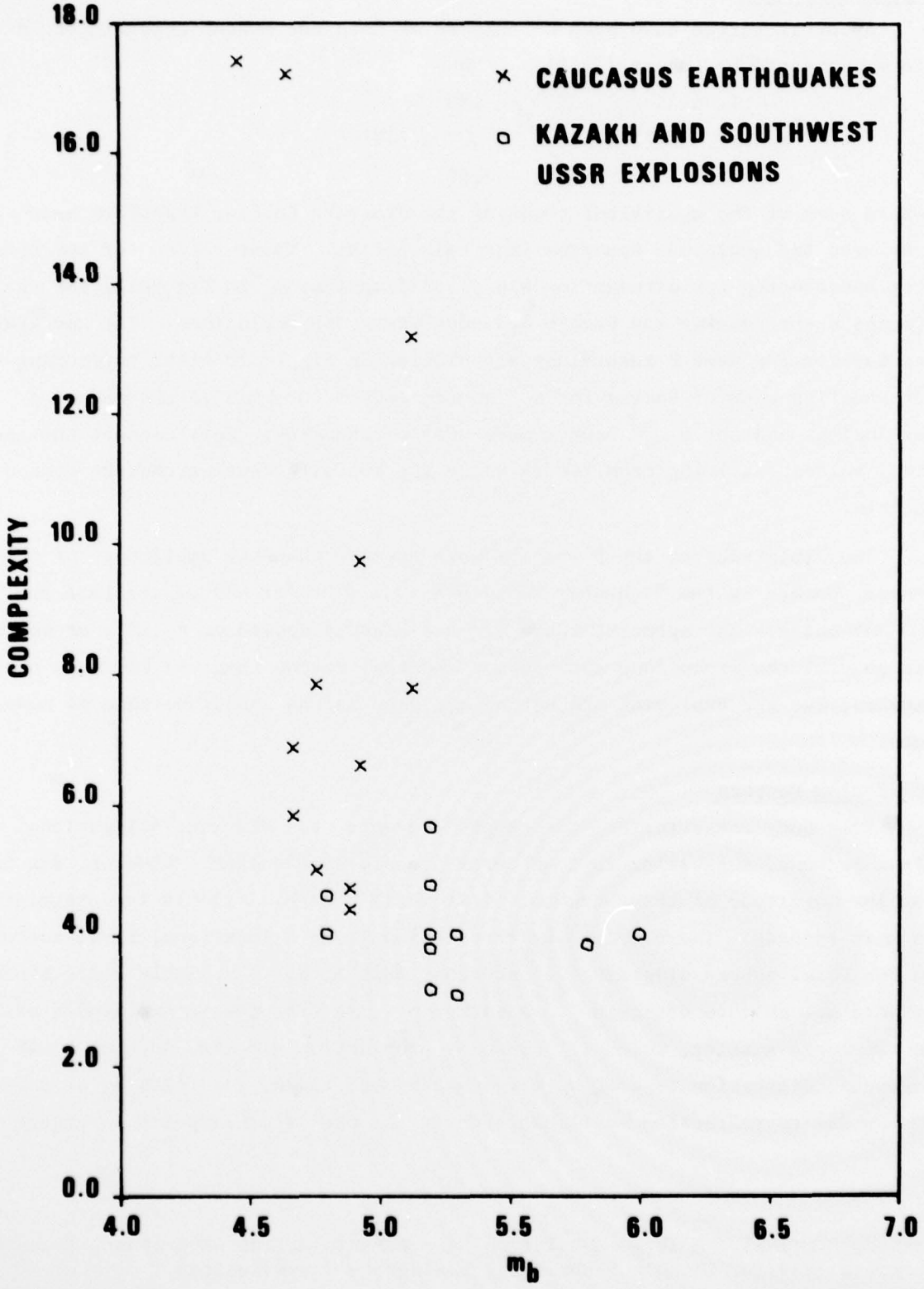

Figure 16. Complexity vs. m_b for Caucasus earthquakes and Kazakh and Southwest USSR explosions from LASA and NORSAR P recordings.

Spectral Ratios

Spectral ratios have been calculated at LASA and NORSAR according to a form suggested by Lacoss (1969)

$$R = \int_{1.55}^{1.95} A(f)df \Big/ \int_{.45}^{.85} A(f)df$$

where sums of the equivalent terms of the discrete Fourier transform have replaced the amplitude spectrum integrals A(f)df. These ratios for the spectra uncorrected for attenuation are plotted against m_b in Figure 17 for the Caucasus earthquakes and Kazakh and southwest USSR explosions. The spectral ratios for the same P recordings are plotted in Figure 18 after correcting for attenuation with t^* values for ω^{-2} source models for both earthquakes and explosions and for a ω^{-3} source model for earthquakes. Bars connect the spectral values resulting from the t^*'s for the two different earthquake source models.

The amplitudes of the P spectra were greater than the amplitudes of the noise spectra in the frequency range 0.4 to 2.0 Hz for all of the LASA and NORSAR beams. The spectral ratio did not clearly depend on m_b, M_s, or depth. In general the explosions show larger spectral ratios than the Caucasus earthquakes, but the explosion and earthquake populations cannot be said to separate.

Radiation Pattern

Some body waves for all the Caucasus events show distinct dilatational first motions, suggesting that these events are earthquakes. However, due to the low magnitude of these events, first motions were difficult to determine on most records. The overlapping compressional and dilatational first motions on the focal sphere diagrams indicate that this is not a reliable discriminant. We were not able to determine a radiation pattern from the LR amplitudes owing to the large scatter, which is caused by propagation effects, such as Q differences, dispersion effects on time-domain amplitudes, and focusing or defocusing due to refraction as illustrated in the predicted raypaths in Figure 13.

Lacoss, R., 1969. A large-population LASA discrimination experiment, Technical Note 1969-24, Lincoln Laboratory, Lexington, Massachusetts.

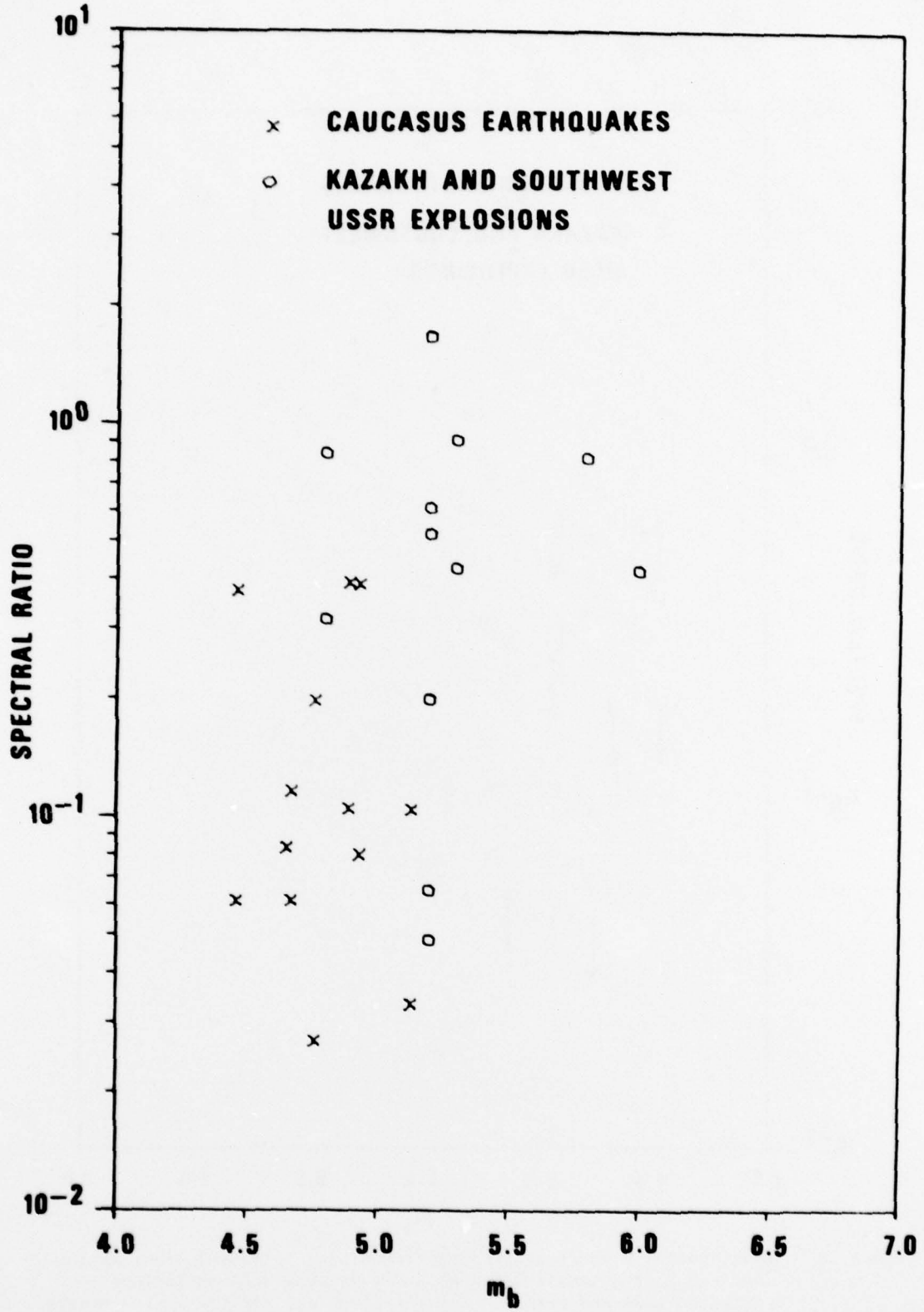

Figure 17. Short-period P spectral ratio uncorrected for attenuation vs. m_b for Caucasus earthquakes and Kazakh and southwest USSR explosions recorded at LASA and NORSAR.

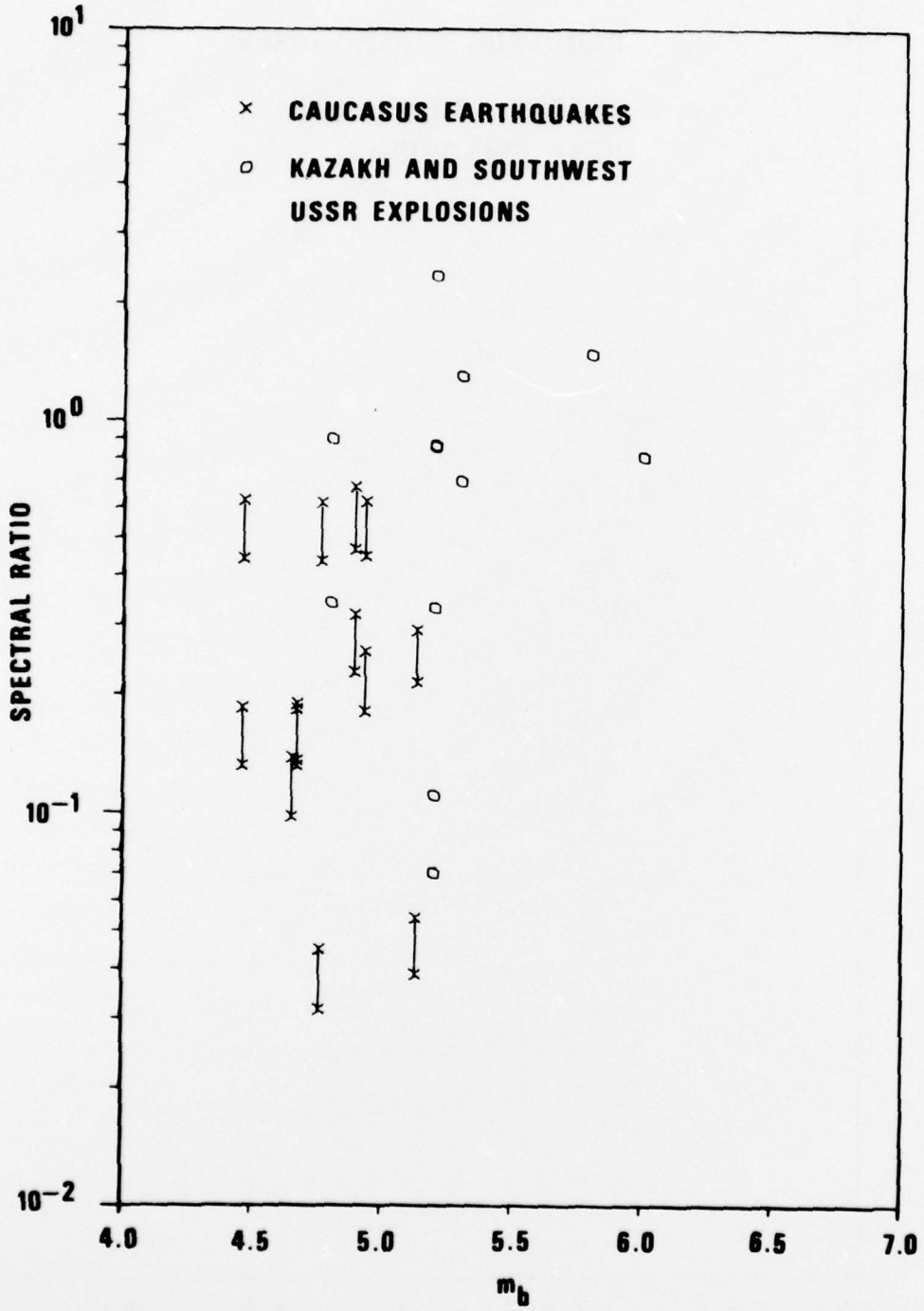

Figure 18. Short-period P spectral ratio corrected for attenuation vs. m_b for Caucasus earthquakes and Kazakh and southwest USSR explosions recorded at LASA and NORSAR. The t* values are for ω^{-2} source models for earthquakes and explosions and ω^{-3} source models for earthquakes.

S/P Excitation

As would be expected for these small magnitude events, there were no short-period S observations from the Caucasus events to determine the ratio of S/P ground displacement. No clear long-period S phases were seen either.

SUMMARY

Eight earthquakes from the Caucasus and eight Kazakh and southwest USSR explosions were examined in a seismic discrimination context. Most of the Caucasus events lie close to major faults observed in satellite photographs. It was impossible on the basis of first motions to determine individual fault-plane solutions due to the small magnitudes of the events, but thrust faulting may be indicated by the composite pattern. We were also unable to determine a radiation pattern from the LR amplitudes, probably due to varying propagation effects. The following characteristics of the Caucasus events indicate that all the events are earthquakes:

- All the presumed earthquakes had apparent pP phases recorded at LASA, NORSAR, or some of the WWSSN stations.
- All the Caucasus events fall above the line $M_s = m_b - 1.5$. The Kazakh and the southwest USSR explosions lie below the line.

Recall that the Caucasus earthquakes were chosen on the basis that they had the lowest M_s values, relative to m_b, in a preliminary survey. We note that shot arrays could be used to raise the M_s of an explosion by about 0.3 M_s units or more, placing it close to the earthquake population studied here.

Complexity, moment vs. corner frequency, and spectral ratio were not particularly useful discriminants in this data set. The low magnitudes of the earthquakes studied here (m_b from 4.46 to 5.13 and M_s from 3.71 to 4.78) made clear discrimination difficult with the available data, except for M_s-m_b data, and probably represent nearly the lowest threshold of multi-discriminant analysis for the source region and stations used in this report. The installation of high-quality SRO stations in Asia will permit the examination of lower magnitude events with multistation short-period data.

REFERENCES

Beliayevsky, N., A. Borisov, I. Valvovsky, and Y. Schukin, 1968, Transcontinental crustal sections of the U.S.S.R. and adjacent areas, Canadian Journal of Earth Sciences, 5, 1967.

Ben-Menahem, A., S. Smith, and T. Teng, 1965. A procedure for source studies from spectrums of long-period seismic body waves, Bull. Seism. Soc. Amer., 55, 203.

Blandford, R. R., and D. Clark, 1975, Variability of seismic waveforms recorded at LASA from small subregion of Kamchatka, SDAC-TR-75-12, Teledyne Geotech, Alexandria, Virginia.

Borusk, A., and V. Shalpo, 1976, Correlation of endogenous processes in the Great Caucasus and adjacent part of the Scythian Platform, in Geodynamics: Progress and Prospects, ed. C. Drake, American Geophysical Union.

Byus, E. I., A. D. Tskhakaya, and M. M. Rubinshtein, 1968. Regional seismic zoning of the USSR: Georgia, in Seismic Zoning of the USSR, edited by S. V. Medvedev, English translation, Keter Publishing House, Jerusalem, Israel.

Dahlman, O., I. H. Israelson, A. Austegard, and G. Hornstrom, 1974, Definition and identification of seismic events in the USSR, Bull. Seism. Soc, Am., 64, 607.

Geller, R. J., 1976. Scaling relations for earthquake source parameters and magnitude, Bull. Seism. Soc. Am., 66, 1501.

Hanks, T., and W. Thatcher, 1972. A graphical representation of seismic source parameters, J. Geophys, Res., 77, 4393.

Keilis-Borok, V. I., 1960. Investigation of the Mechanism of Earthquakes, English translation, American Geophysical Union, Washington, D. C.

Lacoss, R., 1969. A large-population LASA discrimination experiment, Technical Note 1969-24, Lincoln Laboratory, Lexington, Massachusetts.

Lambert, D., D. von Seggern, S. Alexander, and G. Galat, 1969. The LONGSHOT Experiment, Volume II. Comprehensive Analysis, SDL Report No. 234, Teledyne Geotech, Alexandria, Virginia.

Neprochnov, Y., 1968, Structure of the earth's crust of epicontinental seas: Caspian, Black, and Mediterranean, Canadian Journal of Earth Sciences, 5, 1037.

Nowroozi, A., 1971, Seismo-tectonics of the Persian Plateau, Eastern Turkey, Caucasus, and Hindu-Kush Regions, Bull. Seism. Soc. Am., 61, 317.

Ringdal, F., 1976, Maximum-likelihood estimate of event magnitude, Bull. Seism. Soc. Am., 66, 789.

von Seggern, D., and P. Sobel, 1975. Experiments in refining M_s estimates for seismic events, SDAC-TR-75-17, Teledyne Geotech, Alexandria, Virginia.

von Seggern, D., and R. Blandford, 1972. Source time functions and spectra for underground nuclear explosions, Geophys. J., 31, 83-97.